TP7632E

COMMUNICATIONS
RESEARCH
LABORATORY

POLARIMETRIC RADAR FOR PRECISE NAVIGATION (PRAN):

Study of an Experimental System

R. CHO, S. HAYKIN and T. GREENLAY

PREPARED FOR THE
TRANSPORTATION
DEVELOPMENT CENTRE

CA1
DTC 801
86
P56
c.2

of Engineering
er University
ı, Ontario
L8S 4K1

APRIL 1986

86-05784/

TP 7632E

POLARIMETRIC RADAR FOR PRECISE NAVIGATION (PRAN):

Study of an Experimental System

by

R. Cho

S. Haykin

and

T. Greenlay

Communications Research Laboratory
McMaster University

Prepared for the
Transportation Development Centre

April 1986

The contents of this report reflect the views of the contractor and not necessarily the official views or policies of the Transportation Development Centre of Transport Canada.

Un sommaire en français de ce rapport est inclus avant la Table des matières.

PROJECT TEAM

M. Avni	Senior Development Officer Transportation Development Centre
J. Betz	Research Technician Communications Research Laboratory McMaster University
R. Cho	Research Engineer Communications Research Laboratory McMaster University
T. Greenlay	Senior Research Engineer Communications Research Laboratory McMaster University
S. Haykin	Director Communications Research Laboratory McMaster University

REPORT DOCUMENTATION FORM

1. Transport Canada Report No.	2. TDC Project No.	3. Recipient's Catalogue No.
TP7632E	6191	

4. Title and Subtitle	5. Report Date
POLARIMETRIC RADAR FOR PRECISE NAVIGATION (PRAN): Study of an Experimental System	April 1986
	6. Performing Organization Report No.

7. Author(s)	8. Transport Canada File No.
R. Cho, S. Haykin and T. Greenlay	D1460-216

9. Performing Organization Name and Address	10. DSS File No.
Communications Research Laboratory McMaster University 1280 Main Street West Hamilton, Ontario, Canada L8S 4K1	10SD.T8200-4-4505
	11. DSS or Transport Canada Contract No. OSD84-00122

12. Sponsoring Agency Name and Address	13. Type of Report and Period Covered
Transportation Development Centre (TDC) Guy Favreau Complex 200 Dorchester Blvd., West, Suite 601, West Tower Montreal, Quebec, Canada H2Z 1X4	Final Oct 1984 - Mar 1986
	14. Sponsoring Agency Code 6119

15. Supplementary Notes	16. TDC Project Officer
	Micha Avni

17. Abstract

A study to define a set of radar and retro-reflector parameters which satisfy the requirements of an automatic system for accurate navigation in confined waterways is described.

A series of experiments was conducted in the anechoic chamber at the Communications Research Laboratory to determine the reflector parameters. A radar installation and two reflector sites were established on the periphery of Hamilton Harbour. The horizontally and vertically polarized signals from the environment and the reflectors were recorded for analysis to determine the radar parameters.

It was concluded from the experiments that (1) polarization diversity is an effective radar discriminant to combat clutter, and (2) the twist grid reflector provides the basis for the implementation of a system for automatic navigation along a confined waterway.

18. Key Words	19. Distribution Statement
Accurate, Marine, Navigation, Polarization, Precise, Radar, Reflector, Retro, Systems, Twist Grid	Limited number of copies available from the Transportation Development Centre on request.

20. Security Classification (of this report)	21. Security Classification (of this page)	22. No. of Pages	23. Price
Unclassified	Unclassified	61	-

TDC CDT 79-005

FORMULE DE DOCUMENTATION POUR RAPPORT

1. N° du rapport Transports Canada	2. N° de l'étude — CDT	3. N° de catalogue du destinataire
TP7632E	6191	

4. Titre et sous-titre	5. Date du rapport
POLARIMETRIC RADAR FOR PRECISE NAVIGATION (PRAN): Study of an Experimental System	Avril 1986
	6. N° du rapport de l'organisme exécutant
7. Auteur(s) R. Cho, S. Haykin et T. Greenlay	8. N° de dossier Transports Canada D1460-216
9. Nom et adresse de l'organisme exécutant Communications Research Laboratory McMaster University 1280 ouest rue Main Hamilton, Ontario, Canada L8S 4K1	10. N° de dossier — ASC 10SD.T8200-4-4505
	11. N° de contrat — ASC ou Transports Canada OSD84-00122
12. Nom et adresse de l'organisme parrain Centre de développement des transports (CDT) Complexe Guy-Favreau 200ouest, boul. Dorchester, suite 601, tour ouest Montréal, Québec, Canada H2Z 1X4	13. Genre de rapport et période visée Final Oct. 1984 - Mars 1986
	14. Code de l'organisme parrain 6119
15. Remarques additionnelles	16. Agent de projet — CDT Micha Avni

17. Résumé

Ce rapport rend compte d'une étude visant à déterminer les paramètres de fonctionnement d'un ensemble radar/réflecteurs répondant aux exigences d'un système automatique de radionavigation de précision en voies navigables intérieures.

D'abord les paramètres de fonctionnement des réflecteurs ont été déterminés grâce à une série d'expériences menées dans une chambre anéchoique des laboratoires de recherche du ministère des Communications. Ensuite, les chercheurs ont établi un site radar et de réflecteurs à proximité du port de Hamilton dans le but d'enregistrer les signaux à polarisation horizontale et verticale réfléchis par le milieu environnant et les réflecteurs, signaux dont l'analyse devait permettre de déterminer les paramètres du radar.

Les résultats indiquent que: (1) la technique de la polarisation diversité assurait une bonne protection anti-clutter et (2) les réflecteurs à grilles inclinées pouvaient être utilisés comme cheville ouvrière d'un système de navigation de précision en voie de navigation intérieure.

18. Mots-clés	19. Diffusion
Navigation maritime, polarisation, radar, réflecteur, réflecteur à grilles inclinées.	Le CDT dispose d'un nombre limité d'exemplaires.

20. Classification de sécurité (de ce rapport)	21. Classification de sécurité (de cette page)	22. Nombre de pages	23. Prix
non-classifié	non-classifié	61	-

CDT TDC 79-005

ACKNOWLEDGEMENTS

The authors gratefully acknowledge the advice and assistance provided by Jonathan Betz at the Communications Research Laboratory; Jerry DeBoer at the Engineering Machine Shop, McMaster University; Ed Lewis and Trevor Dyas at the Canada Centre for Inland Waters; Gunther Morwald and Kevin Moriarity at Dofasco; Ian Ledingham at the Burlington Recreation Services Department and Ian Noble at the Hamilton Harbour Commissioners.

Jonathan Betz designed and built the interfaces for the data acquisition system, and digitized the data off the RCA recorder. Jerry DeBoer modified the antenna pedestal and constructed the stands for the radar equipment and the mounting brackets for the reflectors. Jerry also fabricated the reflectors and provided much assistance in their installation. Ed Lewis was responsible for providing the use of Inland Waters and its facilities for the radar system and data acquisition. Trevor Dyas installed and modified the radar equipment. Gunther Morwald, Kevin Moriarity, Ian Ledingham and Ian Noble made available the various reflector sites and helped in their selection.

The authors would like to acknowledge the financial assistance provided by NSERC for the purchase of the radar equipment. Finally, the authors would like to thank Micha Avni and the Transportation Development Centre for their assistance over the course of this study.

SUMMARY

This report presents the experiments conducted to study the requirements of an automatic system for precise navigation in confined waterways.

The primary objectives of the study were:

a. To define a set of reflector and radar parameters for the precise navigation system.

b. To verify the acquisition and retention of the reflectors by a scanning antenna.

c. To determine the effects of electromagnetic interference on precise navigation.

In order to achieve these objectives, a radar installation was established at the Canada Centre for Inland Waters in Burlington, Ontario, along with reflector sites at the Dofasco steel foundry in Hamilton and La Salle Park in Burlington. A dual-polarized radar was assembled from off-the-shelf components and reflectors were constructed using data obtained in laboratory tests. The radar was used to illuminate the twist grid reflectors to determine the reflector's ability to rotate the incident polarization and thus distinguish itself from the clutter. The field data collected were analyzed to obtain the reflector and radar parameters, and to determine the effects of electromagnetic interference.

It was concluded from the results that:

a. Polarization diversity is an effective radar discriminant to combat clutter.

b. The twist grid reflector can be easily located by the scanning antenna, even in a very hostile radar environment such as the Dofasco site.

c. Electromagnetic interference does not degrade the target detection capability of the precise navigation system.

d. The twist gird reflector provides the basis for the implementation of a system for automatic navigation along a confined waterway.

In view of the above conclusions, efforts should now concentrate on the development of a prototype version of the system for moving platform tests.

SOMMAIRE

Ce rapport décrit les expériences menées dans le but de déterminer les caractéristiques à exiger d'un système automatique de radionavigation de précision en voies navigables intérieures.

Les principaux objectifs de l'étude étaient de:

a) définir les paramètres de fonctionnement d'un ensemble radar/réflecteurs pour la radionavigation de précision,

b) vérifier les conditions d'acquisition et de maintien dans le champ des réflecteurs par une antenne de balayage,

c) déterminer les effets des perturbations électromagnétiques sur la précision du pilotage.

A cette fin, les chercheurs ont établi un site radar au Centre canadien des eaux intérieures à Burlington (Ontario) et disposé des réflecteurs sur le terrain de la Dofasco à Hamilton et dans le parc La Salle à Burlington. A partir de composants standard, ils ont monté un radar à double polarisation et construit des réflecteurs répondant aux exigences préalablement définies en laboratoire. Par la suite, le radar a été utilisé pour éclairer les réflecteurs à grilles inclinées et déterminer s'ils étaient capables de faire tourner le plan de polarisation de l'onde incidente et d'émerger ainsi du clutter environnant. L'analyse des données recueillies sur le terrain a permis de déterminer les paramètres de fonctionnement des réflecteurs et du radar, et de cerner les effets des perturbations électromagnétiques.

Les résultats indiquent que:

a) la technique de la polarisation diversité assurait une bonne protection anti-clutter,

b) les réflecteurs étaient facilement repérables par une antenne de balayage, même dans un site aussi peu propice à la détection radar que l'usine sidérurgique de la Dofasco,

c) les perturbations électromagnétiques ne diminuent pas les performances de détection du système envisagé,

d) les réflecteurs à grilles inclinées peuvent être utilisés comme cheville ouvrière d'un système de navigation de précision en voies de navigation intérieures.

Compte tenu de ce qui précède, nous considérons que l'on devrait passer à l'étape de la construction d'un système prototype et soumettre celue-ci à des essais sur plate-forme mobile.

TABLE OF CONTENTS

			Page
1.	INTRODUCTION		
	1.1	Background	1
	1.2	Objectives	1
	1.3	Approach	1
2.	TRIHEDRAL TWIST GRID REFLECTOR		
	2.1	Introduction	3
	2.2	Theory of Operation	3
	2.3	Twist Grid Reflector Prototype	3
	2.4	Test Setup	4
	2.5	Test Procedure	4
3.	RADAR RANGE MEASUREMENT		
	3.1	Introduction	8
	3.2	Approach	8
	3.3	Ranging Accuracy	8
	3.3.1	Inherent Range Accuracy of Radar Pulse	8
	3.3.2	Waveform Modelling	9
	3.4	Radar Simulation	10
	3.5	Bias Errors	11
	3.6	Detection Algorithm	12
4.	RADAR INSTALLATION AND REFLECTOR SITES		
	4.1	Radar Facility	16
	4.2	Reflector Sites	16
5.	DATA ACQUISITION SYSTEM		
	5.1	Introduction	22
	5.2	Radar-RCA Interface	22
	5.3	RCA-Ampex Interface	22
	5.4	Ampex-Computer Interface	22
	5.5	AP-HP Data Transfer	23
	5.6	Data Organization	23
6.	DATA COLLECTION AND ANALYSIS		
	6.1	Alignment of Reflectors	25
	6.2	Recording and Sampling of Data	25
	6.3	Reflector Size	26
	6.4	Analysis	26
7.	RESULTS		
	7.1	Twist Grid Reflector	27
	7.2	Target Detection	27
	7.3	Range Accuracy	28
	7.4	Interference Conditions	29
	7.5	Weather Effects	30
8.	CONCLUSIONS		44

REFERENCES

LIST OF ABBREVIATIONS

BIBLIOGRAPHY

LIST OF FIGURES

Figure 1	Top View of Electric Field Components on Twist Grid	6
Figure 2	Cross-Section of Trihedral Surface with Twist Grid	6
Figure 3	Reflector Test Setup	7
Figure 4	Waveform Models	13
Figure 5	Rectangular Pulse	14
Figure 6	Normalized Ambiguity Function	14
Figure 7	Normalized Mean Square Error Function	14
Figure 8	Ground and Slant Range Geometry	15
Figure 9	Block Diagram of the Radar System	17
Figure 10	Radar Components: PPI Displays, Sector Blanking Unit, Transceivers and Rectifiers	18
Figure 11	Parabolic Antenna Dish with Dual, Linear Polarized Feed	19
Figure 12	Dofasco Reflector Site	20
Figure 13	La Salle Park Reflector Site	21
Figure 14	Data Acquisition System	24
Figure 15	Reflector Signal as a Function of Twist Grid-Reflector Separation	31
Figure 16	Reflector Signal as a Function of Azimuth	32
Figure 17	Reflector Signal as a Function of Elevation	33
Figure 18	Horizontally and Vertically Polarized Sweeps of the Dofasco Reflector	34
Figure 19	Horizontally and Vertically Polarized Sweeps of the La Salle Park Reflector	35
Figure 20	Horizontally and Vertically Polarized Sweeps of the Dofasco Site (No Reflector)	36
Figure 21	Horizontally and Vertically Polarized Sweeps of the La Salle Park Site (No Reflector)	37
Figure 22	Scan Converted Image of Radar Coverage Area (Range = 6.20 Km)	38
Figure 23	Scan Converted Image of Radar Coverage Area (Range = 3.17 Km)	39
Figure 24	Target Detection: Vertical Sweeps of the La Salle Park Reflector Site	40
Figure 25	Simulated Sweeps of the Dofasco Reflector	41
Figure 26	Simulated Sweeps of the La Salle Park Reflector	42
Figure 27	Range Accuracy Simulation	43

1. INTRODUCTION

1.1 Background

Since 1978, the Dominion Marine Association (DMA) and the Transportation Development Centre (TDC) have been involved in the testing and development of a marine radar that will aid and enhance precise navigation in confined waterways. In 1980, DMA and TDC conducted a series of trials on a section of the St. Lawrence Seaway near the Ogdensburg/Prescott International Bridge with a Precise Radar Navigation System (PRANS) developed by Associated Controls & Communications, Inc. (ACCI), of Salem, Massachusetts. For a number of technical reasons, the PRANS equipment was not able to match the accuracy and reliability of existing systems [1,2,3]. However, it was concluded that PRANS would be an effective navigational aid if it could be fully developed. The use of passive reflectors would provide increased system reliability as well as economic advantages.

In a study performed for TDC by the Communications Research Laboratory (CRL) in 1983, it was found that the use of polarization diversity and space diversity provided a solution to many of the shortcomings of ACCI's equipment [4]. Subsequent to that study, a trihedral reflector with a twist grid to rotate the polarizaton of the incident radiation was invented and patented by Macikunas, Haykin, and Greenlay at CRL [5,6].

The new passive retro-reflector is an essential element of the Polarimetric Radar for Accurate Navigation (PRAN) system addressed in this report. For the system to succeed, the signal from the reflector must be easily acquired by the ship's radar under the many different conditions encountered along a waterway like the St. Lawrence.

1.2 Objectives

In view of the results of the 1983 study, a follow up study was proposed to look at the various requirements of the precise navigation system and to test the performance of the newly developed polarimetric reflector. The objectives of the present study are:

a. Define a set of reflector parameters, section 7.1.

b. Verify the acquisition and retention of the reflectors by a scanning antenna in an operational environment, section 7.2.

c. Define a set of radar parameters that will satisfy the performance requirements of the precise navigation system, section 7.3.

d. Determine the impact of electromagnetic and other interference conditions on the system, sections 6.4, 7.2, 7.4 and 7.5.

1.3 Approach

In order to study the various aspects of the precise navigation problem, a radar installation and two reflector sites were established on the periphery of Hamilton Harbour. The area around the harbour provided a good cross section of the type of environment a ship

encounters along a typical waterway. The environment ranged from a heavily industrialized area to a lightly wooded area.

A horizontally polarized X-band (Decca) marine radar and an antenna with a dual-polarized feed (manufactured by Andrew Antenna) were used to illuminate the environment. The horizontally and vertically polarized signals were viewed on two plan position indicator (PPI) displays. The signals were also recorded for analysis in the laboratory. To study the parameters for the PRAN system, a radar simulation was used. The simulation modelled the environment and the characteristics of the system using the recorded data. Various parameters in the model were changed to simulate different scenarios. The simulated data were then analyzed to determine the proper parameters for the PRAN system.

The reflector parameters were determined by testing various twist grid reflectors in the anechoic chamber at CRL. The anechoic chamber eliminates the interference of echoes from walls, floor or ceiling with absorbing foam. The recorded field data were used to calculate the required radar cross-section of the reflectors.

2. TRIHEDRAL TWIST GRID REFLECTOR

2.1 Introduction

The trihedral reflector is made up of three mutually orthogonal planes with the property that radiation incident on any one plane undergoes reflection off the remaining two and is redirected back in the direction of the source. The ratio of reflected to incident power density is known as the radar cross-section (RCS). The RCS density is defined as the RCS divided by the area illuminated by the radar. The radar cross-section of a triangular trihedral reflector is given by

$$RCS = 4\pi a^4/3\lambda^2 \tag{2.1}$$

where a is the edge length of the reflector and λ is the wavelength of the incident radiation. Thus a large increase in the radar cross-section can be achieved with a relatively small increase in the edge length. The trihedral reflector also has a wide response, a 3 dB beamwidth of approximately 39 degrees (deg), in both azimuth and elevation.

The new reflector developed at CRL incorporates the ordinary triangular trihedral reflector with a wire grid suspended above one of the reflector planes. This combination produces a rotation of the incident polarization by 90 degrees over a wide range of angles in both azimuth and elevation. For maximum reflection of the signal, the reflector is oriented with the lower plane at 35.26 deg below the horizontal.

The wire grid is a series of closely spaced parallel wires suspended above the reflector surface by a medium with a low dielectric constant. The theoretical relationship between the wire spacing, wire diameter and height off the reflector surface is given by Macikunas [6].

2.2 Theory of Operation

When the wire grid is optimally oriented at 45 degrees to the incident polarization, the horizontal and vertical components of the signal are equal in magnitude. Upon encountering the wire grid, the horizontal component of the incident wave is reflected by the wires while the vertical component continues on through the grid, to be reflected by the underlying surface. With the wire grid positioned approximately $\lambda/4$ above the reflector plane, the vertical component is delayed by $\lambda/2$ or 180 degrees. When the reflected components recombine, the resultant polarization is rotated by 90 deg, Figure 1. Since the lower plane of the reflector is oriented at 35 deg below the horizontal for maximum reflection, the incident polarization does not hit the wire grid at 45 deg. To compensate for this the reflector is rotated about its axis by approximately 15 deg.

2.3 Twist Grid Reflector Prototype

To determine the parameters of the wire grid, a triangular trihedral reflector with an edge length of approximately 0.62 metres (m) was constructed and tested with a variety of grids suspended above the lower face of the reflector. Both the reflector and the grids were manufactured at the McMaster engineering machine shop. The tests were carried out in the anechoic chamber at CRL. The quantity used to evaluate the effectiveness of a grid was the like polarization rejection ratio (LPRR) [6]. This is a measure of the difference between the

like- and cross- polarized signal in decibels (dB). It is also an indication of the efficiency of the wire grid to rotate the polarization of the signal.

The reflector was constructed of aluminum sheets, 1.6 millimetres (mm) in thickness and welded together. The wires of the grid were laid out in individual strands across a backing with a low dielectric constant, Figure 2. A variety of materials were used as the backing, among them foam, plexiglass and styrofoam. It was found that the pouring and curing of the foam disrupted the wire spacing to the extent that the grid was often unusable. In the second method, lines were scored in the plexiglass and the wires were laid in the grooves. The wires were held in place with a fine coat of varnish. This produced a very durable grid but the plexiglass backing was not transparent enough and the results obtained were poor. The best results were achieved with the styrofoam. The wires were placed on the styrofoam and held in place with masking tape. The grid was inserted into the reflector with the wires on the bottom and positioned over the reflector surface with three plastic screws. The distance between the grid and the reflector was varied by adjusting the screws.

2.4 Test Setup

The trihedral twist grid reflector was mounted on a dual axis antenna positioner so that the response of the reflector to changes in the azimuth and elevation could be studied. The bracket mount for the reflector consisted of two flat plates connected by a swivel joint. The flat plates were used to attach the back of the reflector to the antenna positioner while the swivel joint allowed the reflector to be rotated about its axis.

The microwave signals used to illuminate the reflector were supplied by a Hewlett Packard (HP) radio frequency generator, HP-8621B RF Section, in conjunction with a sweep oscillator, HP-8620A, to provide a frequency range from 8 to 11 gigahertz (GHz), Figure 3. The signals were fed into a microwave amplifier, HP-495A, and directed to a horizontally polarized rectangular horn antenna at one end of the anechoic chamber, directly opposite the reflector at the other end. The reflected signals were detected by two identical horns with one rotated 90 deg to receive the cross-polarized signal. The like- and cross-polarized signals were displayed one at a time on the phase-magnitude display, HP-8421A, via the harmonic mixer, HP-8411A, and the network analyzer, HP-8410A. The signal traces were then plotted on a flatbed plotter, HP-7044A.

2.5 Test Procedure

Each grid was tested for its response to changes in the distance between the grid and the reflector surface, rotation about its axis, azimuth and elevation in order to determine a set of reflector parameters that will give the best performance. The elevation and azimuth angles were both initially set to 0 deg. The spacing between the grid and reflector was varied from approximately 1.6 centimetres (cm) to 2.2 cm at 0.1 cm steps with the three adjustment screws. This height has been theoretically calculated to be 1.98 cm [6]. At each height, the reflector was rotated about its axis to find the best orientation. This was done by changing the angle to get the deepest null on the like-polarized return to appear in the neighbourhood of interest, approximately 9.4 to 9.5 GHz, or conversely, to place the strongest signal on the cross-polarized return in the same neighbourhood.

At each height and orientation, three traces were plotted showing the like polarization without the wire grid in the reflector and like and cross polarizations with the wire grid in the reflector. By comparing the plots it was possible to determine the best height and orientation for that particular grid. The reflector was repositioned at these settings and

the remote controlled antenna positioner was used to change the azimuth and elevation angles from approximately −20 deg to +20 deg in 5 deg increments. This allowed the azimuth and elevation beamwidths of the reflector to be determined.

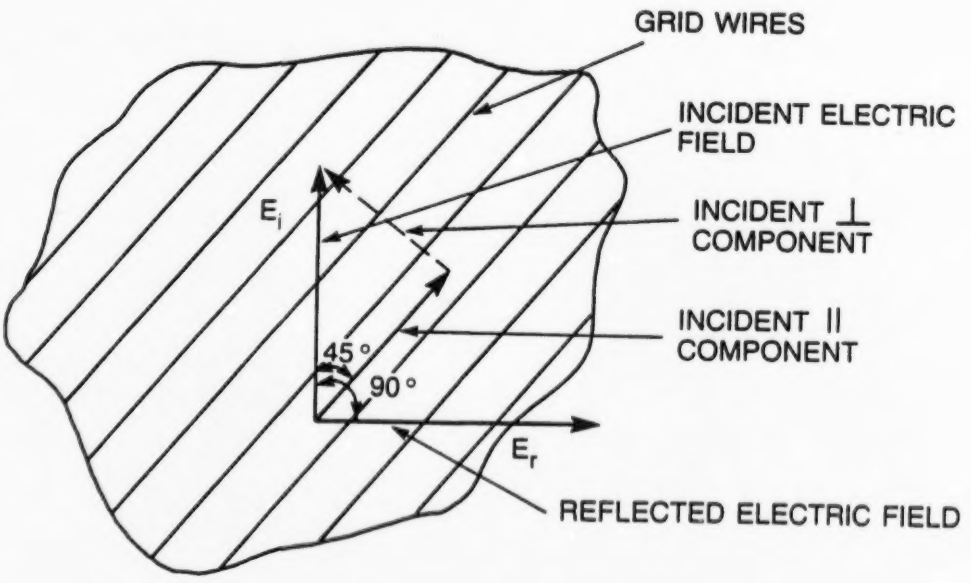

Figure 1 Top View of Electric Field Components on Twist Grid

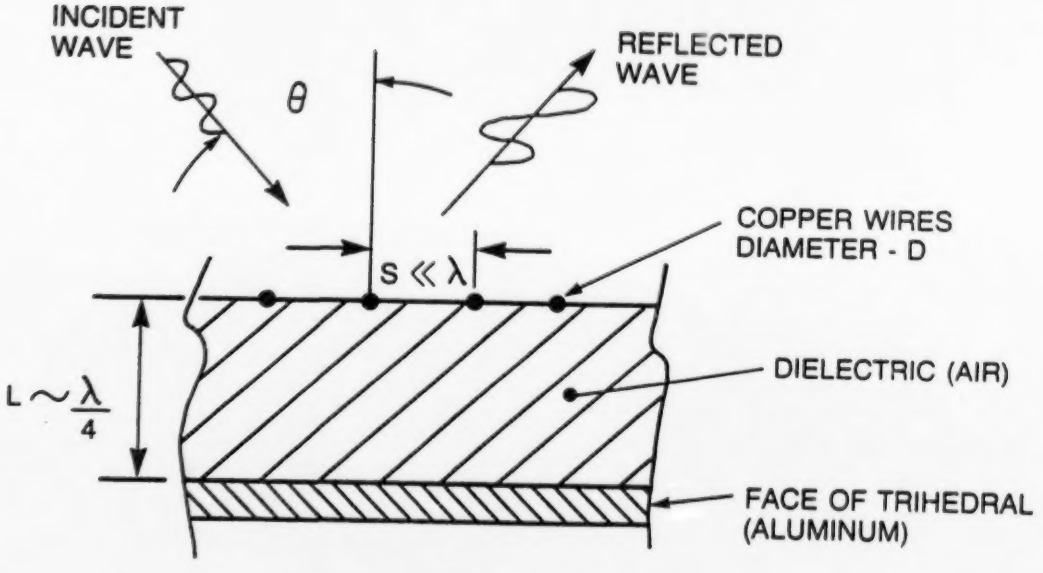

Figure 2 Cross-Section of Trihedral Surface with Twist Grid

(Prepared by Arunas Macikunas)

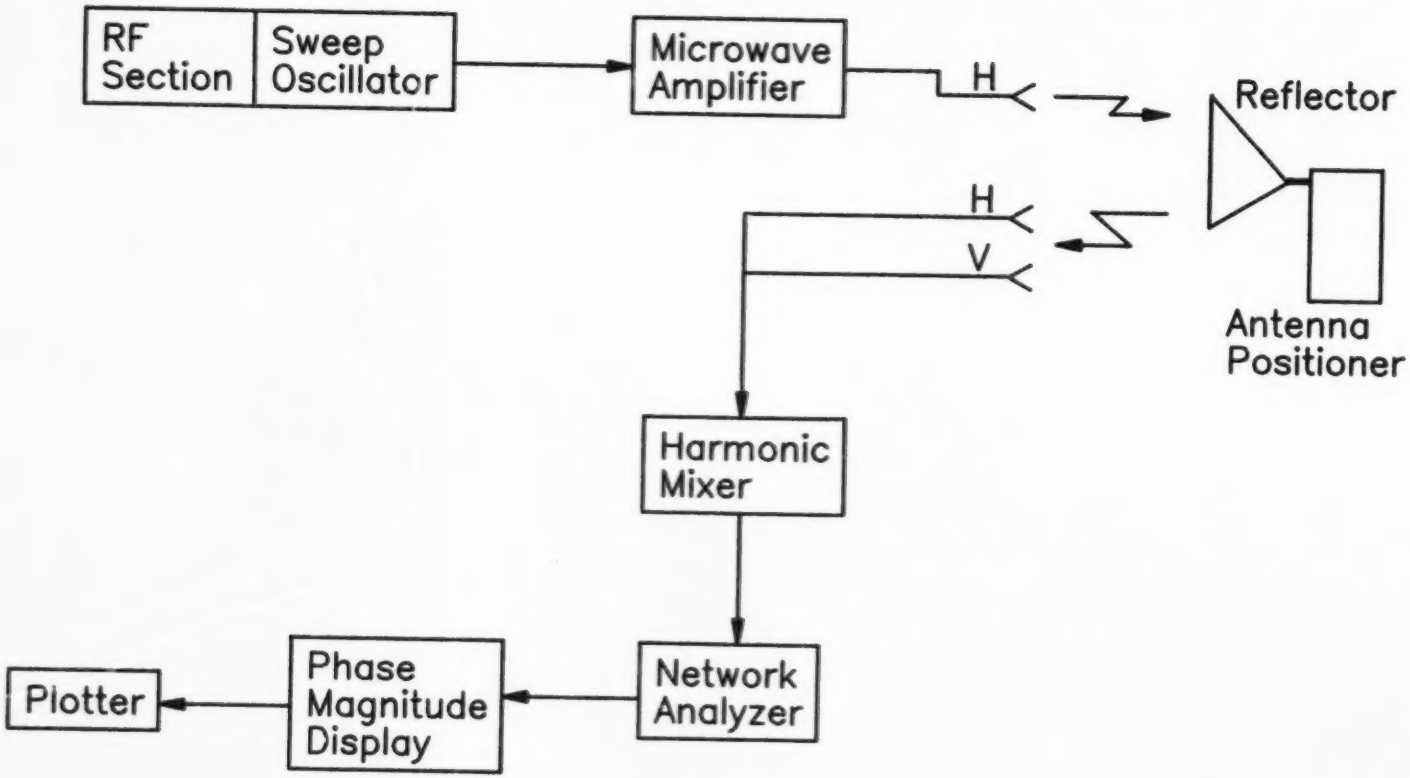

Figure 3 Reflector Test Setup

3. RADAR RANGE MEASUREMENT

3.1 Introduction

The distance, d, to a target as measured by radar is given by the time delay, t, between the transmission of the pulse and the reception of its echo through the equation

$$d = ct/2 \tag{3.1}$$

where c is the speed of light (3×10^8 m/sec). The presence of a target is assumed when the strength of the return signal exceeds a predetermined threshold level. Though it is relatively straightforward to measure the time delay, there are many factors that can distort t. The most significant ones are the radar waveform and the receiver bandwidth. Other factors include the threshold level, amount of noise in the system and the length of the waveguides between the antenna and the receiver. These and other factors will be discussed below.

The range accuracy requirement for the PRAN system has been determined to be 7.5 metres or 50 nanoseconds (ns) for a typical ship of 224 m long, 23 m beam and 8 m draft, navigating a channel 115 m wide [7].

3.2 Approach

Due to the many different types of marine radars in operation, it is not useful to apply the following analysis to one specific radar type nor is it practical to try and cover the full range of radars in use. The approach will be to study the radar ranging problem in general. The first step will involve a theoretical discussion of the effects the radar waveform and receiver bandwidth have on the range measurement. From this evaluation, a waveform of a certain pulse width and rise time will be deduced to satisfy the accuracy requirement. This waveform will then be used in the radar simulation to verify the observations made in step one. In step three, other errors such as the length of the waveguides that could affect the time delay will be discussed.

Strictly speaking, the term, 'accuracy' is used when only one target is present, and 'resolution' when more than one target is present. In general, high resolution implies high accuracy but the converse is not necessarily true. In this report, no distinction is made between the two terms.

3.3 Ranging Accuracy

For every radar waveform there is a limit to how accurately the distance to a target can be measured. This limit is an inherent property of the radar pulse, and it cannot be improved upon without altering the waveform used. The inherent range accuracy of a waveform is defined to be the width of the output pulse at half amplitude (-3 dB). The following development is that given by Bird [8].

3.3.1 Inherent Range Accuracy of Radar Pulse

The concept of inherent range accuracy of a radar pulse is the amount of change a target with time delay t and doppler ω must undergo before a difference in the time delay exceeds a preset threshold. If the target has a time delay and doppler offset of (x,y) at position

1 and $(x-\tau, y+\omega)$ at position 2, then the difference between the two received signals $f(t-x, \omega_0 + y)$ and $f(t-x+\tau, \omega_0+y+\omega)$ must exceed a minimum value before they are seen to be different. The doppler offset is a frequency shift of the signal spectrum due to the radial velocity of the target. The mean square error (MSE), e^2, between the two signals is given by

$$e^2 = \int_{-\infty}^{\infty} [f(t-x, \omega_o + y) - f(t-x+\tau, \omega_o+y+\omega)]^2 dt \tag{3.2}$$

or

$$e^2/2E = 1 - |\chi(\tau, \omega)| \cos[(\omega_o+y+\omega)\tau - \mathrm{Arg}(\chi(\tau, \omega))]/2E \tag{3.3}$$

This represents an oscillating function bounded by the envelope $1 - |\chi(\tau,\omega)|/2E$. The inherent range accuracy of the pulse is obtained by setting the left hand side of Equation (3.3) to .5 (−3 dB). This gives

$$.5 = 1 - |\chi(\tau,\omega)|/2E$$

or

$$|\chi(\tau,\omega)|/2E = .5 \tag{3.4}$$

The quantity $\chi(\tau,\omega)$ is a function of the time delay and doppler offset and is known as the ambiguity function. It should be noted that τ and ω define a coordinate system relative to the target and not the radar. The ambiguity function is given by the cross correlation of the transmitted pulse with a reflected version of itself as found in a matched receiver. For stationary targets, $\omega = 0$ and Equation (3.4) becomes

$$|\chi(\tau,o)|/2E = .5 \tag{3.5}$$

This gives the time delay t or distance the target must be moved before the change in the return signal exceeds 0.5.

The bandwidth of the receiver is important not only to the ranging problem but also target detection. The narrower the transmitted pulse, the broader will be the main lobe of its frequency spectrum. If the receiver bandwidth is not wide enough to pass these frequency components, the net result is that of transmitting a longer pulse with a loss in range accuracy. Also, the signal-to-noise ratio (SNR) is lowered if the receiver bandwidth is too wide or too narrow relative to the signal bandwidth. This will degrade the target detection performance of the system. To take full advantage of the accuracy inherent in a pulse and to maximize the signal-to-noise ratio for target detection, the receiver is assumed to be a matched receiver with a bandwidth of approximately $1/\tau$.

3.2.2 Waveform Modelling

The waveform normally used in marine radars is the rectangular pulse. The ideal pulse is one with a flat top and zero rise and decay times. This is impossible to realize since a zero rise time requires infinite bandwidth. For practical systems, the rise time is nonzero and the top of the pulse will not necessarily be flat.

To model a realizable rectangular pulse, several assumptions are made:

1. The rise times of the leading and trailing edges of the pulse are equal.

2. The rise time can be approximated by a gaussian function.

3. Maximum fluctutation across the top of the pulse is 10%.

4. The rise time is very much less than the pulse width.

The equation used to model the rectangular pulse is given by

$$\mu(t) = 1 - .5\,[1 - \cos(\pi p t)] \qquad 0 \le |t| \le \tau/2$$

$$= \exp\,[-.5\,(.1t/\tau)^2] \qquad |t| \ge \tau/2,\ p = 0, 2, 4 \tag{3.6}$$

The variance, $\sigma^2 = .01t^2/15.24$, of the gaussian function is set so that for a rise time of t ns, the gaussian function is approximately zero after t ns. The value p varies the number of oscillations across the top of the pulse to simulate the amplitude fluctuations of an actual pulse. Figure 4 shows a 50 ns pulse with a 20 ns rise time for the three p values. Changing the number of oscillations across the top of the pulse for a fixed pulse width and rise time widens or narrows the ambiguity function. This results in a slightly different range accuracy for each of the p values. The difference between the minimum value (most accurate) and the maximum value (least accurate) is less than 1 ns. In all calculations the maximum or least accurate value is used.

To calculate the inherent accuracy, a pulse is generated using Equation (3.6), Figure 5. The cross correlation of the pulse is taken to give the ambiguity function, Figure 6. The intersection of the normalized MSE function, Equation (3.5), with the line .5 gives the inherent accuracy of the pulse, Figure 7.

3.4 Radar Simulation

The derivation of the pulse accuracy in the previous section did not take into account the effects of range attenuation, clutter and system noise on range accuracy. A simulation is used to verify the range accuracy of the waveform and to determine other parameters such as antenna beamwidth.

A simple model has been developed based on the actual terrain surrounding the radar site. A suitable description of the terrain was obtained by digitizing a map of the area. This approach does not take into account extended clutter or shadowing effects due to the elevation of the terrain. This does not present a problem since the reflectors are assumed to have a clear line of sight to the radar, so that only the water surface in front and a small land area behind each reflector are of significance.

In the simulation, the area of interest is divided into resolution cells that are mapped into the corresponding cells on the digitized map to distinguish between the sea and land clutter. The clutter is modelled by assigning an average radar cross-section to each cell. The RCS is given by the product of the RCS density for the cell, the area of the cell and the grazing angle of the pulse. The radar cross-sections are then scaled according to the statistics used to describe the clutter. Rayleigh distributions are used for the sea and rain clutter, and a log-normal distribution is used for the land clutter. The reflectors are assumed to be non-fluctuating point targets.

The radar antenna is assumed to have a fan beam in elevation and to scan continuously in azimuth over the coverage area. The antenna motion is assumed frozen

between the transmission and reception of a pulse since the angle between sweeps is much smaller than the beamwidth of the antenna. The antenna power pattern in azimuth is approximated by a gaussian function. The antenna pattern weighting is carried out by convolving the antenna pattern with the RCS samples lying between the half-power beamwidth.

The received signal, S, from a rectangular pulse is approximated by

$$S(\tau, \omega) = \sum_k V_k \chi(\tau - \tau_k, \omega - \omega_k).$$

The quantity V_k is a scale factor that takes into account the range attenuation, the antenna pattern and the RCS of the resolution cell. This can be simplified by noting that for a narrow pulse, the doppler resolution is the inverse of the pulse width. With stationary targets and small doppler offsets from the clutter, the doppler velocity of all the scatterers can be set to zero. This gives

$$S(\tau) = \sum_k V_k \chi(\tau - \tau_k).$$

The thermal noise power, N, of the system is given by

$$N = kTBF$$

where k is Boltzmann's constant (1.38 joules/degree), T is the receiver temperature, B is the receiver bandwidth, and F is the system noise figure. The receiver bandwidth is the inverse of the pulse width.

To verify the range accuracy of the pulse, it must be shown that the pulse width is narrow enough so that resolution cells bordering the target do not include a significant amount of the target signal.

3.5 Bias Errors

There are two conditions that can introduce a significant error into the range measurement and must be compensated for. In a system where high precision is required, the length of the waveguide running between the antenna and the receiver is important. The increase in time delay is equal to the length of the waveguide between the antenna and receiver.

The second condition is a result of the geometry of the problem, Figure 8. If the antenna is high above the reflector and the reflector is close to the ship, there is a significant difference between the antenna-reflector distance (slant range), y, and ship-reflector distance (ground range), x. Assuming the antenna has an elevation beamwidth of 2a, the minimum distance the reflector can be to the ship and still be seen by the antenna is

$$y = H/\sin(a) \quad \text{and} \quad x = H/\tan(a).$$

The difference between y and x is

$$e = y - x = H[1/\sin(a) - 1/\tan(a)].$$

If a = 10 degrees, then e = .0875H. Depending on H, the height of the antenna above the reflector, a large error could result. The error decreases as the distance between the ship and

reflector increases. But for a small separation distance, such as in docking maneuvers, this error is large. For example,

a = 10 degrees,	H = 20 m,	e = 1.75 m	(23.3% of 7.5 m)
a = 10 degrees,	H = 25 m,	e = 2.19 m	(29.2% of 7.5 m)

Another condition that can potentially degrade range accuracy in a high-precision system is the pulse-to-pulse variations in the pulse width, amplitude and timing caused by equipment instability.

3.6 Detection Algorithm

The algorithm implemented for target detection is based on the following assumptions:

a. At least five echo pulses are received from each reflector.

b. The echo pulses from the reflectors are stronger than the clutter.

c. The reflectors are located close to the water's edge.

The first assumption can be easily realized with little or no modification to existing systems. The second assumption is a direct result of the twist grid reflectors. The third assumption follows from the geometry of the problem and is intended to reduce processing time and false target detections since clutter, like large steel structures, that produce strong horizontally polarized echoes are more likely to be located away from the shoreline.

In the algorithm, an array is used to store the most recent 5 sweeps. The oldest sweep is discarded as a new one is moved into the array. If all five values with the same sample number (range) exceed a preset threshold, a target is assumed to be present. This is a form of pulse-to-pulse integration and is known as the sliding-window detector. The range is calculated from the sample number and the rate at which the data was digitized.

The azimuth of the target is determined by locating the sweep with the largest value at the corresponding sample number. This method is called beam splitting. When the range and azimuth of the target have been determined, the 5 sample values used to make the identification are reset to zero to avoid the possibility of a second detection of the same target.

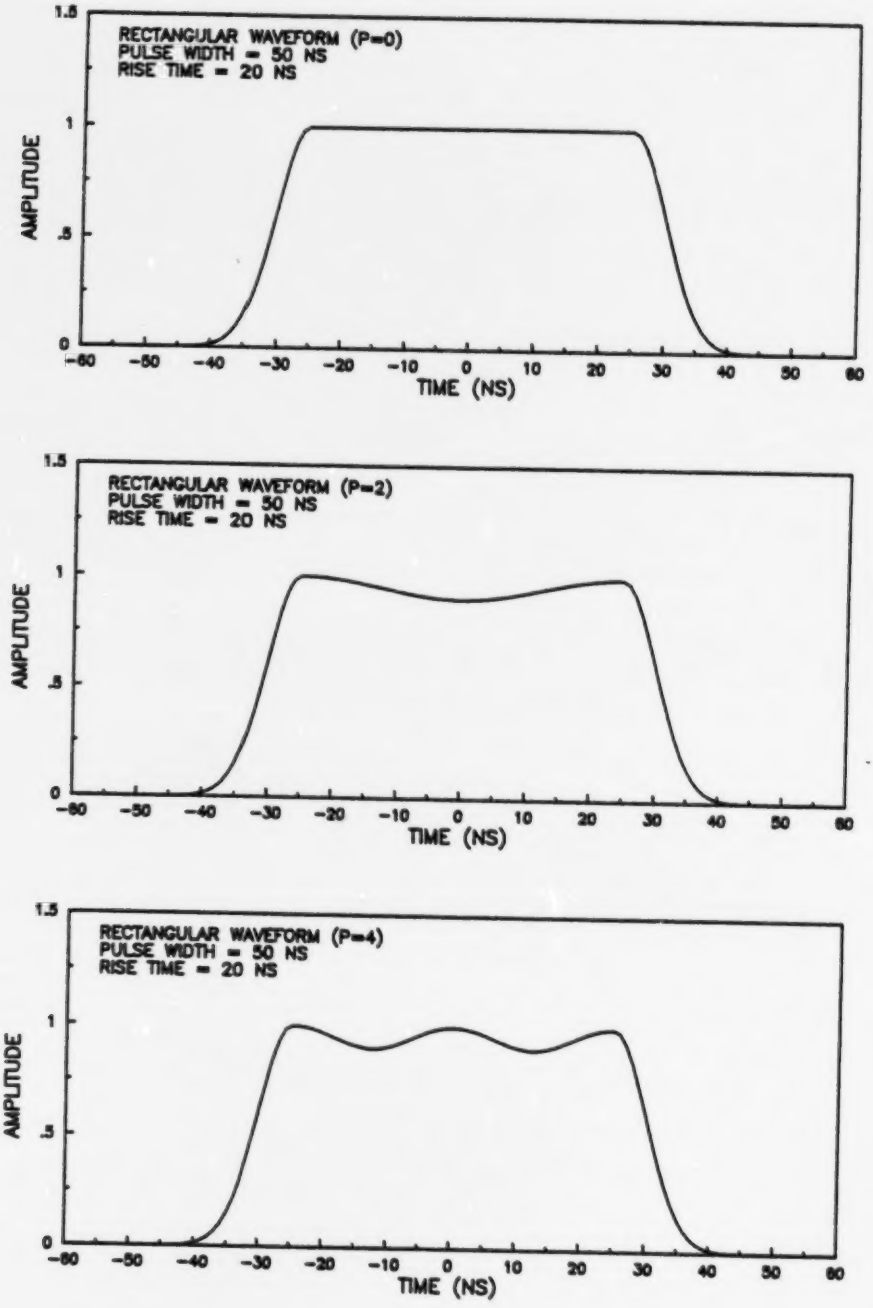

Figure 4 Waveform Models

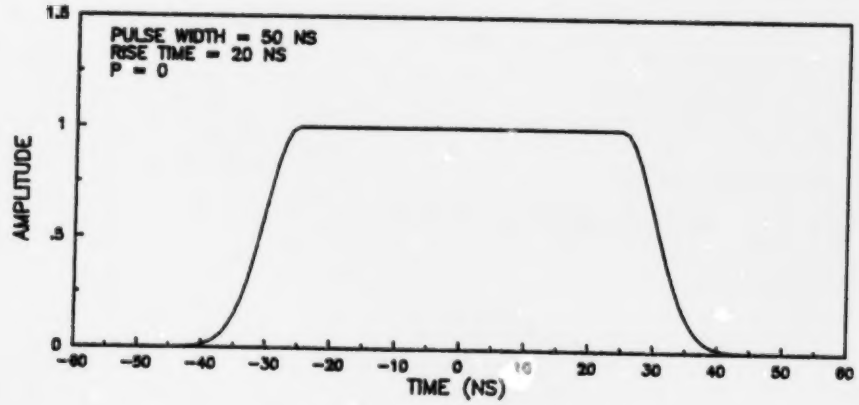

Figure 5 Rectangular Pulse

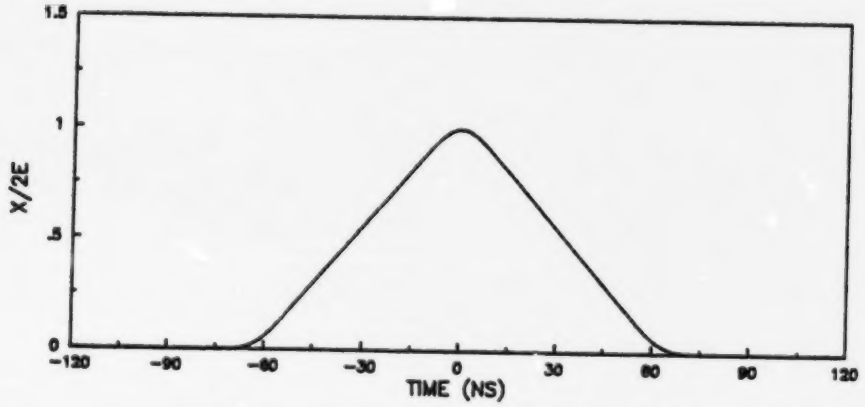

Figure 6 Normalized Ambiguity Function

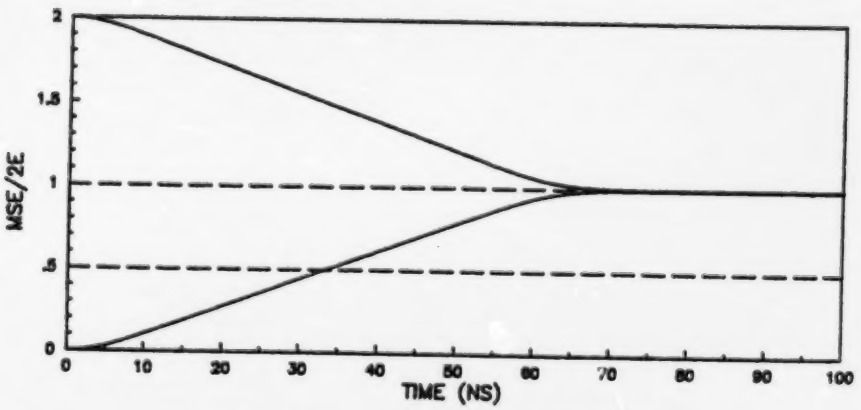

Figure 7 Normalized Mean Square Error Function

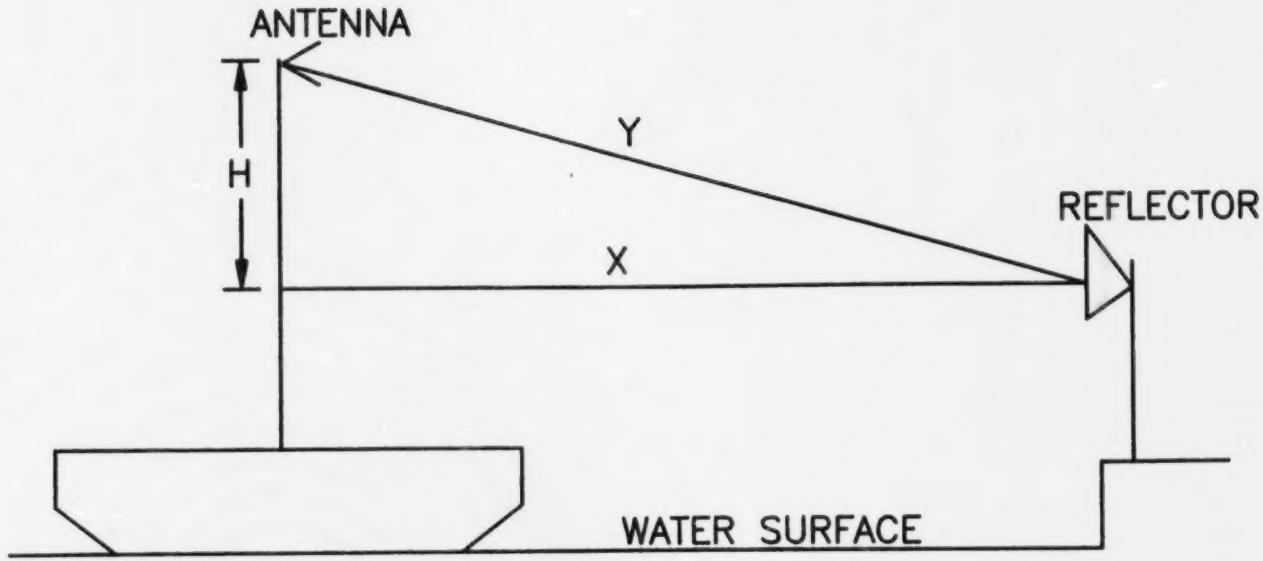

Figure 8 Ground and Slant Range Geometry

4. RADAR INSTALLATION AND REFLECTOR SITES

4.1 Radar Facility

The radar system was assembled from off the shelf components. The system is a RACAL/DECCA RM1229, 3 cm, *X*-band marine radar. The principal components are two 12" PPI displays, two transceivers, a turning unit equipped with a three phase synchro, a sector blanking unit with an azimuth digitizer, a Kevlin Microwave dual channel rotary joint, and a 1.2 m parabolic dish with dual, linear polarized feed from Andrew Antenna, Figures 9 to 11.

The system is located in the northwest stairwell at the Canada Centre for Inland Waters (CCIW) in Burlington. The antenna and its pedestal are mounted on the roof of the stairwell with WR-90 waveguide connecting it to the transceivers in the stairwell below. The system is approximately 43 metres above the harbour with the Burlington Skyway 340 m to the east. Radar coverage in one direction is blocked by an elevator shaft. It is planned to maintain this system in operational status in order to continue polarimetric experiments.

One of the two transmitters was used to illuminate the harbour and the horizontally and vertically polarized images were displayed on the two PPI's. The three phase synchro was used to provide azimuth information to the sector blanking unit which inhibited pulse transmission for part of every scan. This was necessary to prevent signals reflected off the elevator shaft from appearing on the displays. The sector blanking unit was used to reduce the area of coverage to 180 degrees so that only the harbour and areas to the west of the Burlington Skyway were illuminated.

4.2 Reflector Sites

Three reflector sites were initially chosen around Hamilton Harbour, all with a clear line of sight to the radar. The three sites were the Dofasco Steel foundry, Centennial Dock, and La Salle Park in Burlington. However, due to time constraints, the Centennial Dock site was not used, and reflectors were installed and tested only at Dofasco and La Salle Park.

The Dofasco site, Figure 12, was chosen because it presented an environment that is as hostile as any that would be encountered along a waterway. The site is approximately 2270 metres from the radar at CCIW with the reflector mounted on a steel tower. The tower is the same as the one used in the earlier study [4]. The tower is on a concrete platform 10 metres offshore. In the vicinity of the reflector are large piles of raw materials, steel towers and vehicular traffic. Further back from the reflector are the blast furnaces and other large structures. A large freighter was moored several hundred metres west of the reflector site at the time of the study. Due to the weight of the reflector used in this study, the track erected on the tower for the last study was removed to accommodate the clamps and brackets that were needed to hold the reflector.

The La Salle Park site, Figure 13, is approximately 3100 m from the radar and is more typical of the type of environment likely to be encountered by a vessel navigating a waterway. A steel post 3.7 m in height and 8.8 cm in diameter was installed by the Burlington Recreation Services Department for the purpose of this study. The post is located by the edge of the water. A small hill rises behind the site and most of the trees and shrubs in the area were bare during the course of the experiments. Further along the shore, floating docks used during the summer time were stacked on shore providing a visible target to the radar.

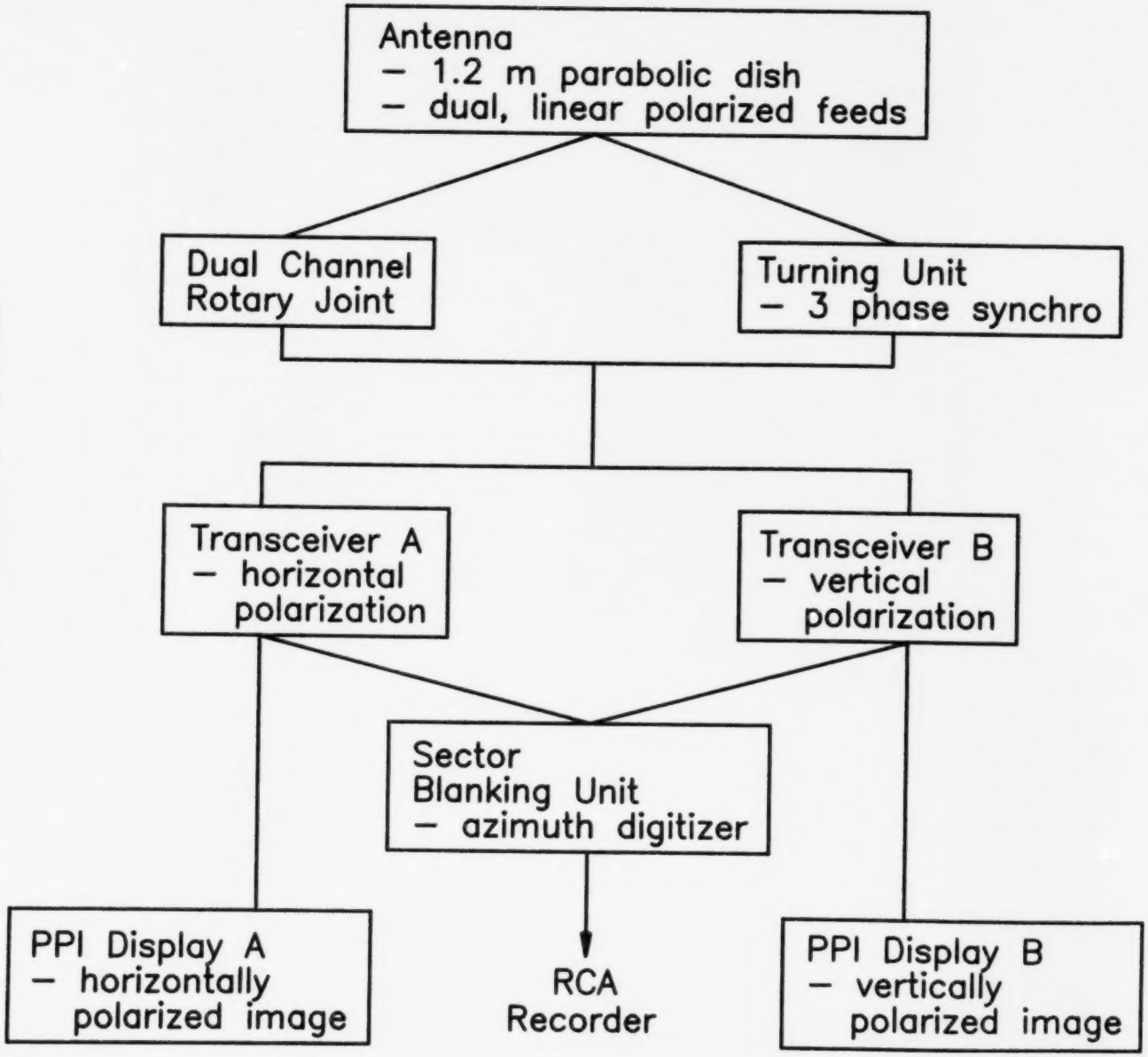

Figure 9 Block Diagram of the Radar System

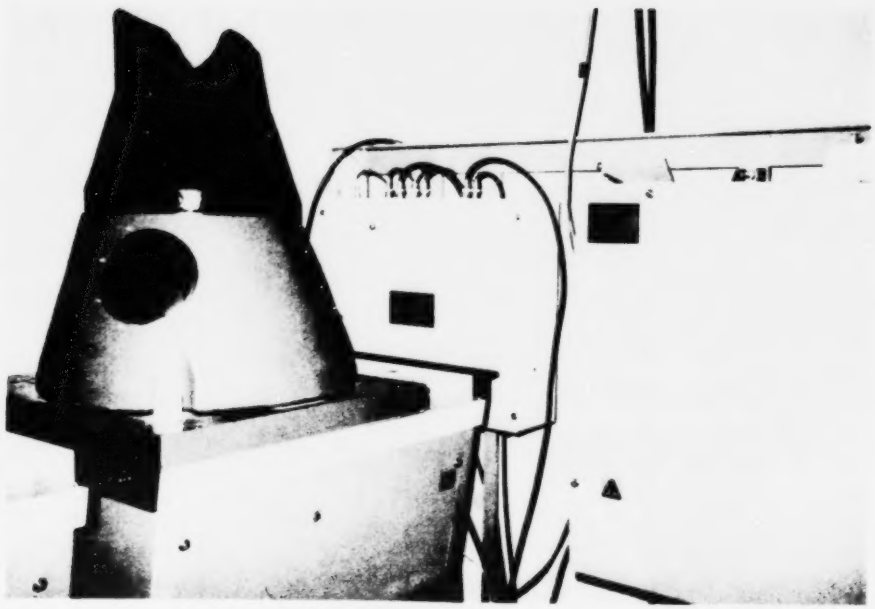

L-R: PPI Display, Sector Blanking Unit,
Transceiver

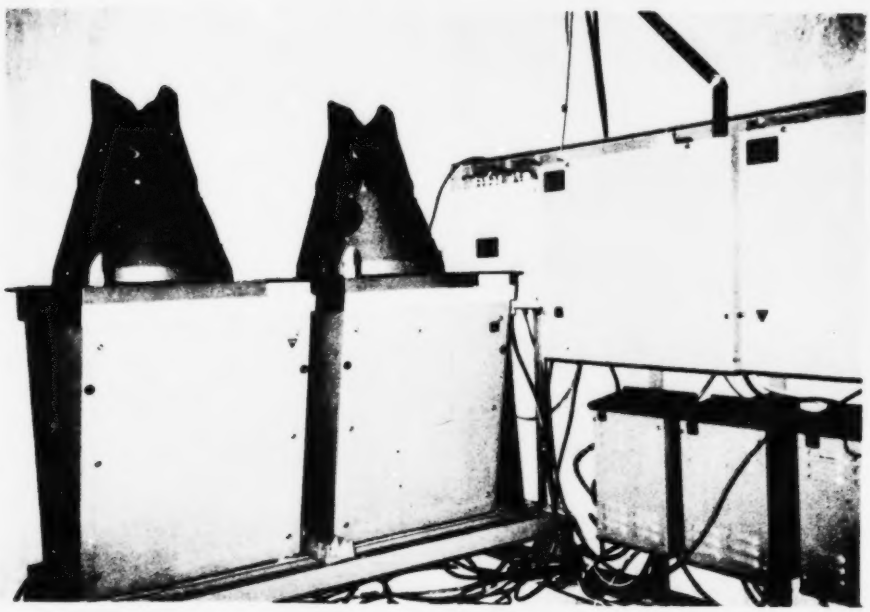

Figure 10 Radar Components: PPI Displays,
Sector Blanking Unit, Transceivers
and Rectifiers

Figure 11 Parabolic Antenna Dish with Dual, Linear Polarized Feed

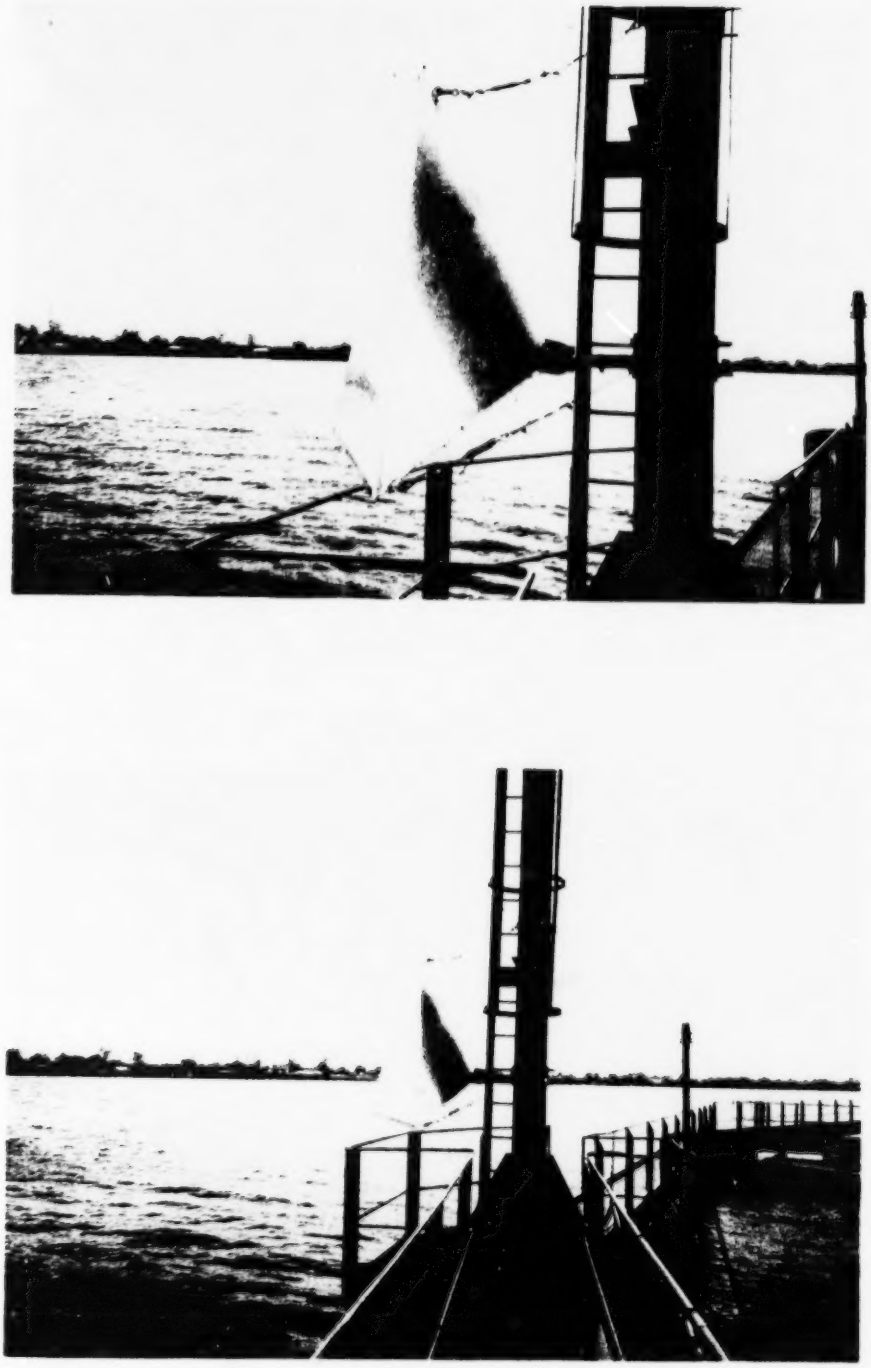

Figure 12 Dofasco Reflector Site

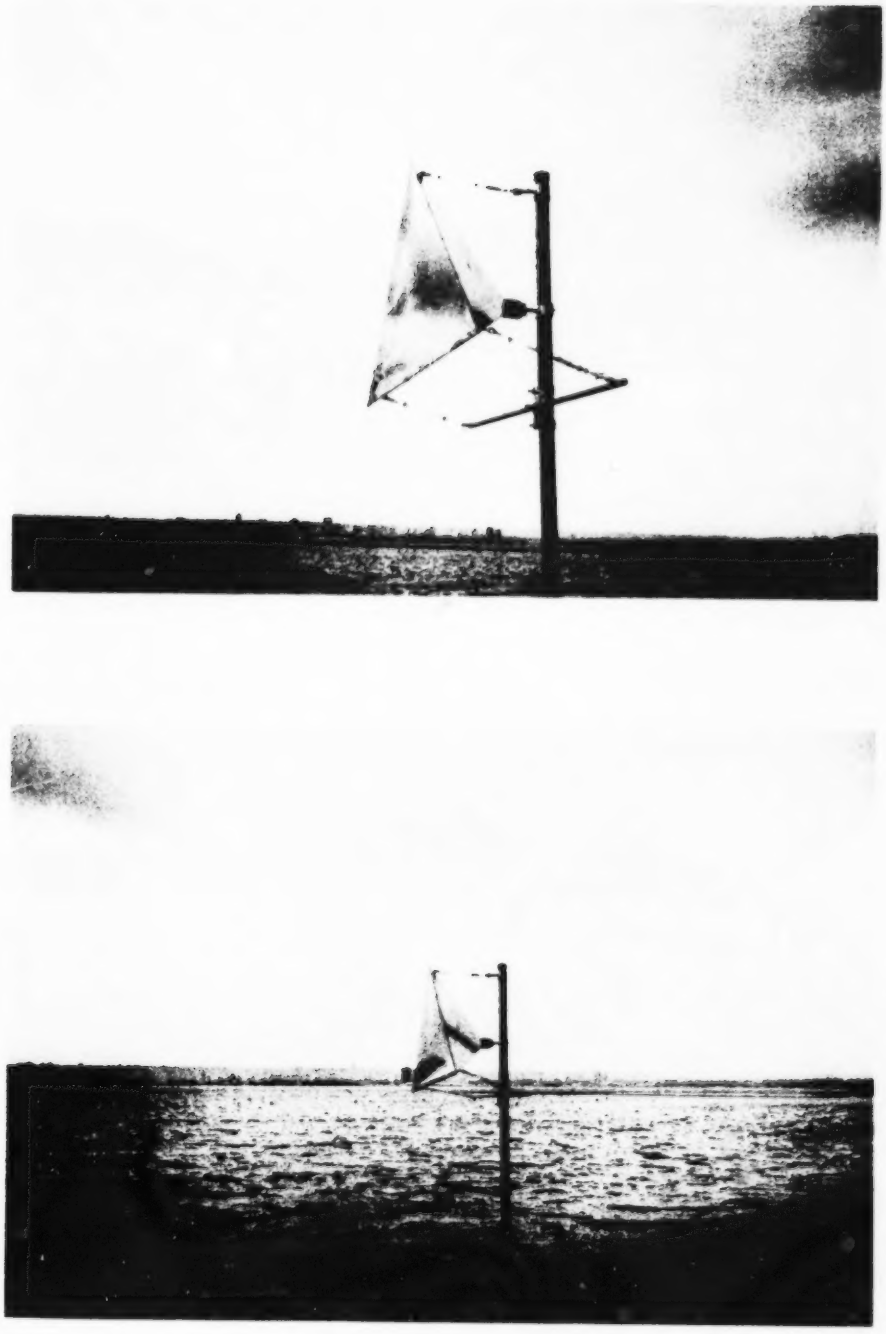

Figure 13 La Salle Park Reflector Site

5. DATA ACQUISITION SYSTEM

5.1 Introduction

The data acquisition system consists of the radar unit, an RCA ADVISER analog recorder, an Ampex AHBR-1728 digital recorder and the Hewlett Packard HP1000 computer with three interfaces connecting the various components, Figure 14. These specialized interfaces were designed and built at CRL. The system is designed to record the horizontally and vertically polarized signals simultaneously as well as the absolute azimuth for each sweep on the RCA recorder. The data cannot be transferred directly into the HP1000 computer due to the high output rate of the RCA, 12.1 megahertz (MHz). The input rate of the HP1000 is approximately 60 kilohertz (KHz). An intermediary is required to reduce the data transfer rate to a level acceptable to the HP1000. Therefore, the information on the RCA is first digitized and recorded on the Ampex digital recorder before being transferred to the HP1000 computer.

5.2 Radar-RCA Interface

The RCA recorder has two video and two auxiliary channels. The horizontally and vertically polarized signals are recorded simultaneously on the video channels, while the absolute azimuth and zero range marks are recorded on the auxiliary channels. The azimuth from the sector blanking unit represents the position of a sweep as a value between 0 and 4095. Each increment increases the angle by 0.088 deg. A zero range mark in the form of a rectangular pulse is sent from the interface to one of the auxiliary channels at the start of every pulse transmission. This is used by the RCA-Ampex interface to initiate the sampling process.

5.3 RCA-Ampex Interface

The analog signals on the RCA are sampled at the rate of 12.1 MHz and recorded on the Ampex. The zero range mark for each sweep is used to ensure the sampling process begins at the same point or range on every sweep. The digitized data is in the form of 8-bit samples with values ranging from 0 to 255. Each sample corresponds to a range of 12.4 m or 82.6 ns.

For each sweep, the first ten samples are ignored. The azimuth information along with a total of 1200 range samples/channel are digitized. The data are transferred to the Ampex in 16-bit words. Each word, excluding the azimuth, consists of a sample from each of the two video channels.

5.4 Ampex-Computer Interface

The Ampex recorder on play back is slowed down to give an average data transfer rate into the computer of approximately 50 KHz. The data are transferred in 32-bit words by multiplexing two 16-bit words together. This is to take advantage of the 38-bit word structure of the Floating Point System (FPS) AP-120B array processor (AP). The azimuth is multiplexed with a 16-bit code word to distinguish it from the sweep data. The AP main data memory is used strictly as a high-speed data buffer.

The transfer of data between the interface and the AP is co-ordinated by the FPS general programmable input-output processor (GPIOP) residing in the AP. A running total of the number of words transferred is stored in one of the GPIOP registers. After every 7212 words, the value in the register is written to the AP. This value is used to check whether any data have been over-written.

5.5 AP-HP Data Transfer

The array processor has two memory boards of 65536 38-bit words each. Only 32 bits of each word are actually used. Each sweep in the AP is made up of the azimuth and 600 sweep data words because of the 4 to 1 multiplexing for a total of 601 32-bit words. Each AP memory board is filled with a maximum of 108 sweeps or 64908 words. The memory board being written is changed every 64908 words. Simultaneously, data are retrieved from the AP and written to the HP disk in blocks of 12 sweeps or 7213 32-bit words (7212 data words plus 1 check word) using EXEC calls for fast transfers. Nine EXEC writes are required to empty one AP memory board.

5.6 Data Organization

Data are taken off the Ampex one scan at a time. This is the equivalent of twenty AP memory boards. The start of each sweep is located by searching for the code word in bits 16 to 31. The azimuth in bits 0 to 11 is written to the two files for the horizontal and vertical data. The next 600 data words are made up of two samples from each of the horizontally and vertically polarized images. These are separated and placed in the corresponding data files.

Only half a scan, corresponding to the harbour and areas west of the Burlington Skyway, is required. In absolute azimuth, this represents the sweeps from 19.78 to 199.78 degrees. Sweeps outside of this region are ignored.

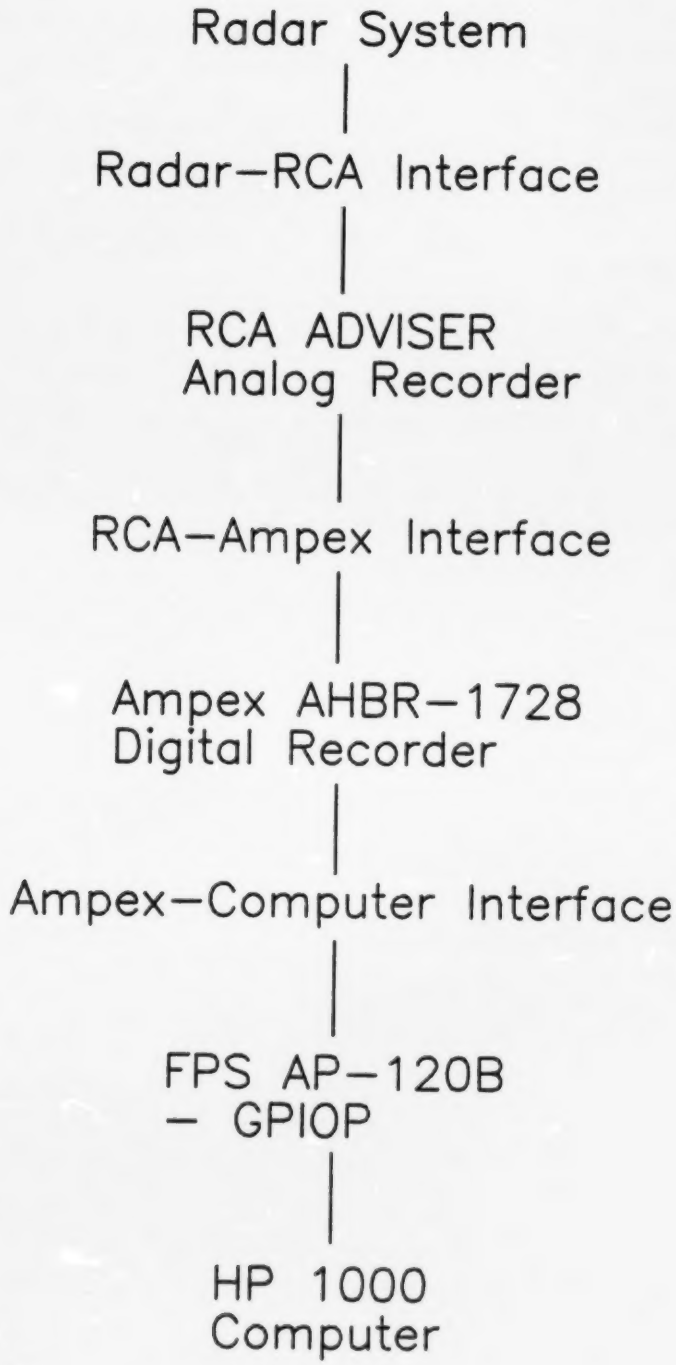

Figure 14 Data Acquisition System

6. DATA COLLECTION AND ANALYSIS

6.1 Alignment of Reflectors

A twist grid reflector was installed at each of the two sites, Dofasco and La Salle Park. The alignment procedure followed was to have an observer at the radar facility relate the change in intensity of the reflector signals to the people in the field as the reflector was rotated through various angles. Portable radios, borrowed from CCIW, were used to provide communications between the radar observer and the field party.

The elevation angle and tilt of the reflector (rotation about the axis) were initially set to the values obtained during the tests in the anechoic chamber at CRL. The reflector was then raised and lowered in height until the maximum signal was observed on the PPI. The reflector was fixed at this height. The tilt, azimuth and elevation angles were then varied individually so as to produce the strongest signal possible on the PPI display.

This method of determining the strongest signal by the PPI intensity is suboptimal because the scanning antenna (one scan every 2 seconds) and the lingering phosphor effect on the cathode tube combine to make such an observation difficult. The correct procedure would have been to disconnect the antenna turning unit, aim the antenna at the reflector, lock it into position and observe the signal amplitudes on an oscilloscope. However, weather conditions prevented this method from being used. For the purpose of this study, the data collected using the above procedure were adequate.

6.2 Recording and Sampling of Data

Due to a number of constraints, the data acquisition system did not perform precisely as that described in Chapter 5. A one microsecond pulse was used in order to maintain the pulse repetition frequency (PRF) at 850 cycles. The PRF of 3400 cycles associated with the 50 nanosecond pulse was too high for the radar-RCA interface.

The horizontally and vertically polarized data had to be recorded sequentially rather than simultaneously because of problems with one of the auxiliary channels of the RCA analog recorder. Consequently, one of the video channels had to be used to record the zero-range marker. As well, problems with the memory buffers on the RCA-Ampex interface allowed 1000 samples to be digitized instead of the proposed 1200. However, at a maximum sampling rate of 12.1 MHz, 1000 samples correspond to a range swath of 12.4 Km. That is well outside of the 9 to 10 Km range swath requirement proposed for the navigation system.

A jitter problem associated with the zero-range mark was eventually reduced to an acceptable level. However, as a result, various sweeps in the data collected are out of step by 1 to 2 range samples.

It should be emphasized that the above difficulties with the data acquisition system are minor in nature. They were not resolved prior to data collection due to time constraints.

6.3 Reflector Size

Initially, reflectors with an edge length of 0.62 m were used. These produced a reasonably strong signal that was adequate for the La Salle Park site, but clutter from the Dofasco site produced return signals of approximately the same magnitude. To over-power the clutter, vertical constellations of these small reflectors were used. It was observed that at least three small reflectors at each site would be required, with each reflector positioned at a maximum in the vertical interference pattern. Due to the height of the post at La Salle Park, the third reflector had to be positioned so close to the ground that its contribution was negligible.

Next, a metal rod with brackets was constructed to mount the three reflectors in a horizontal array. The array was tested at one of the maximums in the interference pattern with mixed results. The individual reflectors were found to be sensitive to minor changes in azimuth, elevation and tilt.

It was decided to use single reflectors at each site but with a larger radar cross-section. From the field data collected using the smaller reflectors, it was determined that reflectors with an edge length of approximately 1.1 m would be required. A reflector of this dimension was constructed and tested at Dofasco with poor results. Closer examination of the reflector revealed that the aluminum used was not heavy enough and because of the increased size, the three sides flexed and were not exactly orthogonal to each other. This problem was resolved and good results were obtained by doubling the thickness of the aluminum sides to 3.13 mm.

6.4 Analysis

The data recorded were digitized and organized into files for analysis. The data were first displayed on the Ramtek graphics system in B-scan format to detect any tape burst errors that are characterized by bright, broken streaks. These were removed by resetting the higher order bits of those words to zero. The parameters of interest were then extracted from the processed data to be used in the simulation. These parameters are the land and sea RCS densities, the Faraday factors (amount of depolarization caused by the land, sea and rain clutter), and the conversion efficiency of the twist grid reflectors.

A one microsecond pulse was used in the recordings and the data were digitized at a rate of 12.1 MHz to give 12 samples per pulse. Each sweep consisted of 1001 samples with the azimuth information contained in the first sample. The maximum of every 12 samples, corresponding to the peak of the pulse, was used in the calculations. Consecutive pulses were then integrated to give the average amplitude for the region. The radar equation was used to obtain the average RCS density from the amplitude. The Faraday factors were found by taking the ratio of the vertical to horizontal RCS densities.

The land clutter was divided into two types, heavily industrialized and wooded areas, and the RCS density was determined for each terrain type. The conversion efficiency of the reflectors was estimated from the radar equation using the amplitude of the return signals.

From the field data processed, it does not appear that electromagnetic interference will present a problem to target detection. The interference appears as long, high intensity streaks that can start and stop at any point along a sweep. However, this is confined to one sweep at a time. Target detection schemes based on two or more target echoes for identification would not mistake interference for a target.

7. RESULTS

7.1 Twist Grid Reflector

The results of the tests performed on the twist grid reflector in the anechoic chamber are given in Figures 15 to 17 for a wire diameter of 0.045 mm and a wire spacing of 5.5 mm. Figure 15 shows the effects of varying the spacing between the wire grid and reflector surface. Each plot has three traces, R, L and X corresponding to the reflector without a grid, and the like and cross polarizations of the reflector with a grid. As the height is increased from 1.6 cm to 2.1 cm, the separation between the like and cross polarizations reaches a maximum of approximately 18 to 20 dB in the region of 9.3 to 9.5 GHz. The maximum separation is reached at a height between 1.9 to 2.0 cm. The difference between the R and X traces is about 1 dB, implying that the wire grid has a conversion efficiency of about 79%.

Figure 16 gives the azimuth performance of the reflector as it is rotated from -10 degrees to $+10$ degrees. The plots show that the deep nulls in the like-polarized returns, L, are reduced as the reflector is moved off 0 degree. At ± 10 degrees, the separation between the like- and cross-polarized returns is still about 10 dB. Also quite apparent is that as the azimuth angle is increased, the conversion efficiency of the wire grid goes down. At ± 10 degrees, the separation between R and X is about 2 to 3 dB.

Figure 17 gives the performance of the reflector as it is rotated in elevation from -10 degrees to $+10$ degrees. At ± 10 degrees, the separation between the like- and cross-polarized signals is between 8 to 10 dB. The conversion efficiency is down about 4 dB or 60%.

Due to the symmetrical nature of the trihedral reflector, the azimuth and elevation performance of the twist grid reflector should be very similar. The fact that the traces are different indicates a problem with the alignment of the test equipment and not with the reflector. From the plots it is apparent that the azimuth and elevation beamwidths of the twist grid reflector are about 20 degrees with a polarization rejection ratio of 18 to 20 dB in the region of 9.3 to 9.5 GHz.

7.2 Target Detection

The horizontal and vertical sweeps corresponding to the strongest returns from the two reflectors are shown in Figures 18 and 19. The vertical sweeps for the two sites without the reflectors are shown in Figures 20 and 21. The ability of the reflectors to rotate the incident polarization and stand out against the ambient clutter is evident. Even in a radar environment as hostile as that found at Dofasco, the untrained eye can easily locate the reflector. Figures 22 and 23 present the horizontally and vertically polarized images in scan converted format. The vertically polarized image was obtained by blanking out pixels with intensity level less than 184. This is equivalent to reducing the gain on the PPI display. The photographs show that the reflectors produce a signal stronger than any clutter in the coverage area. The plots and the photograph demonstrate clearly the effectiveness of using polarization diversity as the radar discriminant to combat clutter.

By studying the individual sweeps at each reflector site, it was possible to determine the location of each reflector in terms of the sweep and sample number.

Site	Sweep	Sample #	Amplitude
Dofasco	147	183	184
La Salle Park	750	251	187

The detection algorithm was applied to the field data with the number of required target echoes reduced from 5 to 3 because of the jitter problem. As well, the threshold level had to be lowered to 120. The following targets were detected.

Site	Sweep	Sample #	Amplitude
Dofasco	147	183	184
La Salle Park	750	251	187
La Salle Park	752	251	161
La Salle Park	755	250	177

A closer examination of the sweeps in the neighbourhood of the La Salle Park reflector, Figure 24, shows that had sweep 751 not been shifted, the threshold value could have been raised to eliminate the false targets. Also, in the absence of jitter, the number of echoes required for target detection, 5, would have eliminated the false targets. This shows that even a relatively unsophisticated algorithm can be used in locating the targets because of the ability of the reflectors to stand out against clutter.

7.3 Range Accuracy

Using the procedure and waveform model outlined in Sections 3.3.1 and 3.3.2, the inherent range accuracy was calculated for a number of waveforms with different pulse widths and rise times. For each pulse width and rise time, three range accuracy values were obtained corresponding to $p = 0, 2, 4$. The least accurate value, $\max[p = 0, p = 2, p = 4]$, was taken. The table below gives the values for a 40 ns pulse with rise times from 1 to 10 ns.

Rise Time (ns)	Range Accuracy (ns)
1	40.8
2	41.7
3	42.5
4	43.4
5	44.2
6	45.1
7	46.0
8	46.9
9	47.7
10	48.6

From this table a rectangular pulse of 40 ns with a rise time of 10 ns is sufficient to give a range accuracy of 7.5 metres. Computer simulation was used to test this waveform in the presence of clutter and noise.

The other parameters used in the simulation were calculated from the field data and are given below.

Site	RCS Density (dB)	Faraday Factor
Dofasco	−10.6	0.01
La Salle Park	−27.7	0.01
Sea	−64.6	1.00

Conversion efficiency of reflectors = 0.7

The Faraday factor for the La Salle Park site was found to be about 1%. Due to extensive shadowing and variability caused by the structures at Dofasco, it was not possible to obtain a consistent value for the Faraday factor. Instead, the one obtained for the La Salle Park site was used. The return from the water was of the same order of magnitude as the system noise. For this reason the Faraday factor has been set to 1, i.e. equal strength for the horizontally and vertically polarized echoes.

The above parameters were tested by generating simulated traces of the two reflector sites, Figures 25 and 26; these results are in general agreement with the field data, Figures 18 and 19. Comparing the two sets of plots it must be remembered that shadowing effects were not considered in the simulation model.

A simulation was performed for a target located at the Dofasco site using a pulse width of 40 ns and a rise time of 10 ns. The results are given in Figure 27. The top plot is a partial trace of the simulation results. The bottom plot is an expanded view of the area around the target. From the bottom plot it can be seen that only three points, corresponding to the peak and midpoints of the pulse are above the 3 dB line. Thus a detection algorithm based on the leading edge measurement technique would result in an accuracy of no worse than 7.5 metres.

Applications of the detection algorithm to simulated and field data have shown that consistent results are achieved by requiring five target echoes to exceed a preset threshold for target identification. For an antenna scanning rate of 30 revolutions per minute (rpm) and a PRF of 800, an azimuth beamwidth of 1.5 to 2 degrees is required.

To compensate for the pitching and rolling motion of the ship and for docking maneuvers, the elevation beamwidth must be broad. An elevation beamwidth of 15 to 20 degrees is sufficient; most marine antennas fall into this range.

7.4 Interference Conditions

The returns of a ship's radar signals as reflected by the retro-reflectors will not interfere with the navigation system of another ship due to the nature of the reflectors. Radiation incident on the retro-reflector is reflected back in the direction of incidence. For the returns of one ship's radar signals to interfere with another ship, both ships' antennas will have to be directed at the reflector at approximately the same incidence angle. Given the unsynchronized nature of the antennas, this scenario is highly unlikely.

The temporary loss of one reflector through blocking from view by a passing ship can be resolved by requiring that four reflectors be visible at all times. The ship's position can be determined from the three remaining reflectors. An alternative would be to require the tracking algorithm be robust enough to handle the temporary loss of one signal and extrapolate the ship's current position based on two reflectors and the ship's last computed position.

7.5 Weather Effects

During the course of the experiments, it was observed that snowfall had no appreciable effect on the performance of the reflectors. No data on the effects of rain clutter were collected due to the weather conditions. However, it is planned to maintain the radar system in operational status to continue polarimetric experiments and rain clutter data will be collected when weather conditions permit.

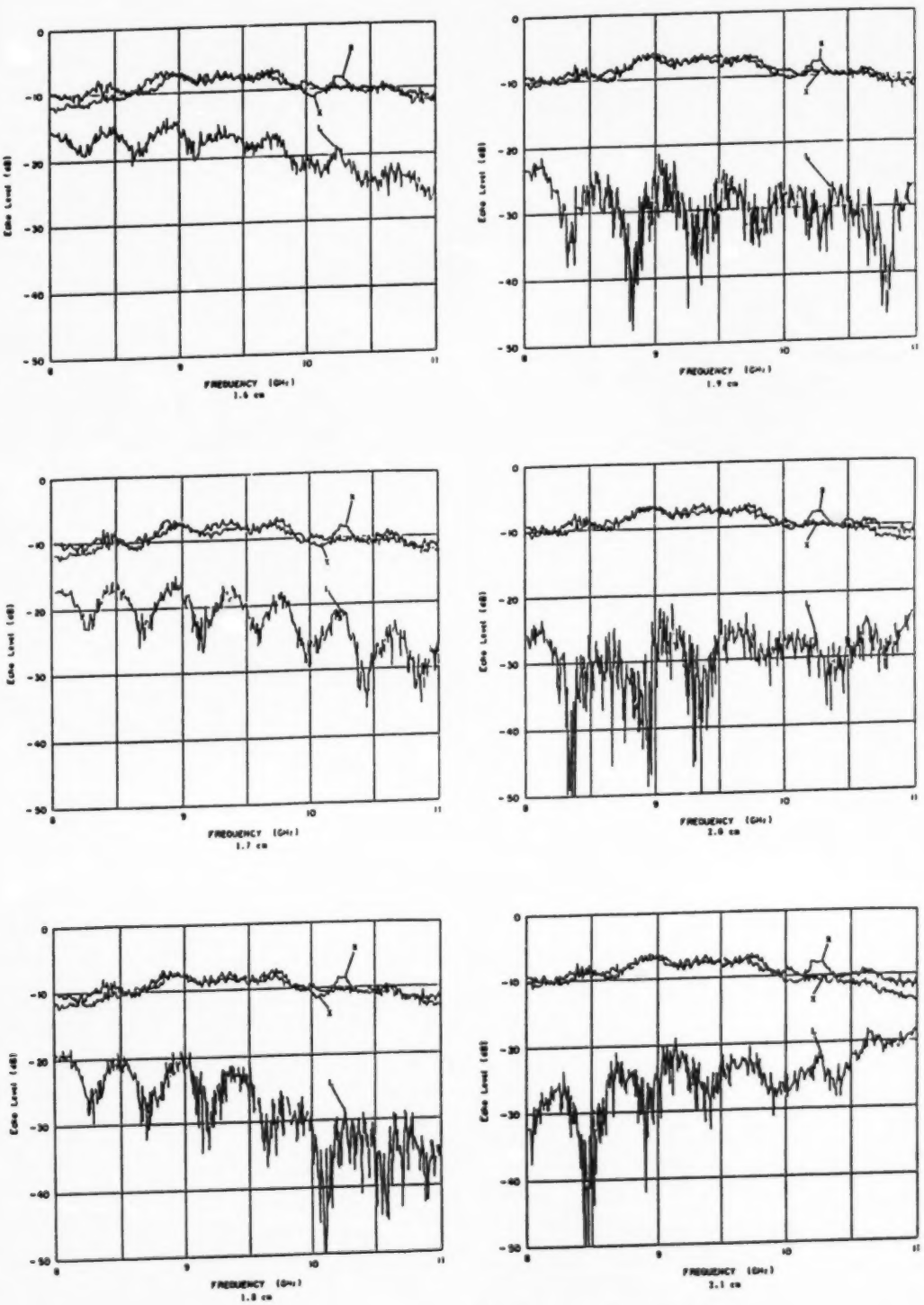

Figure 15 Reflector Signal as a Function of Twist Grid-Reflector Separation

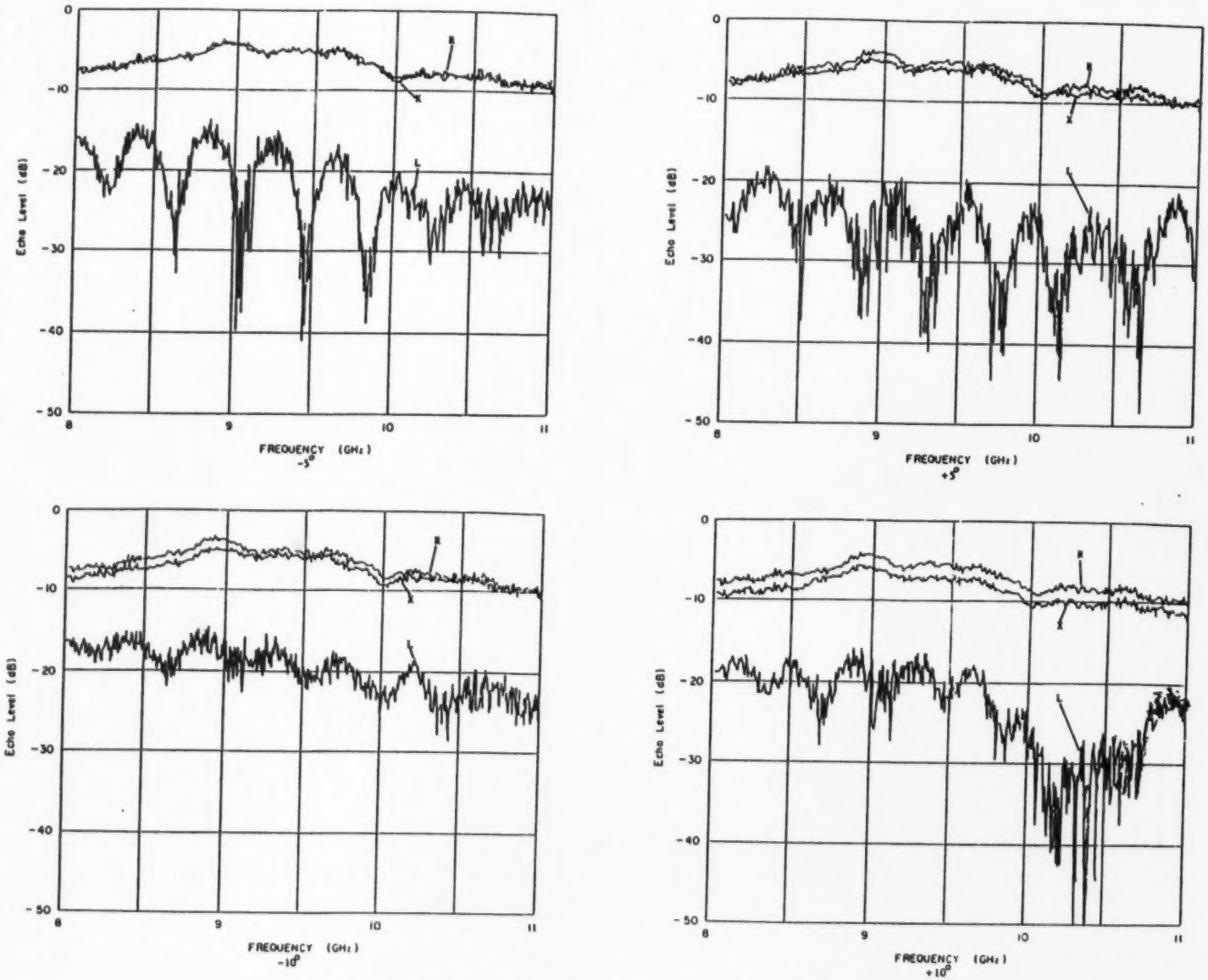

Figure 16 Reflector Signal as a Function of Azimuth

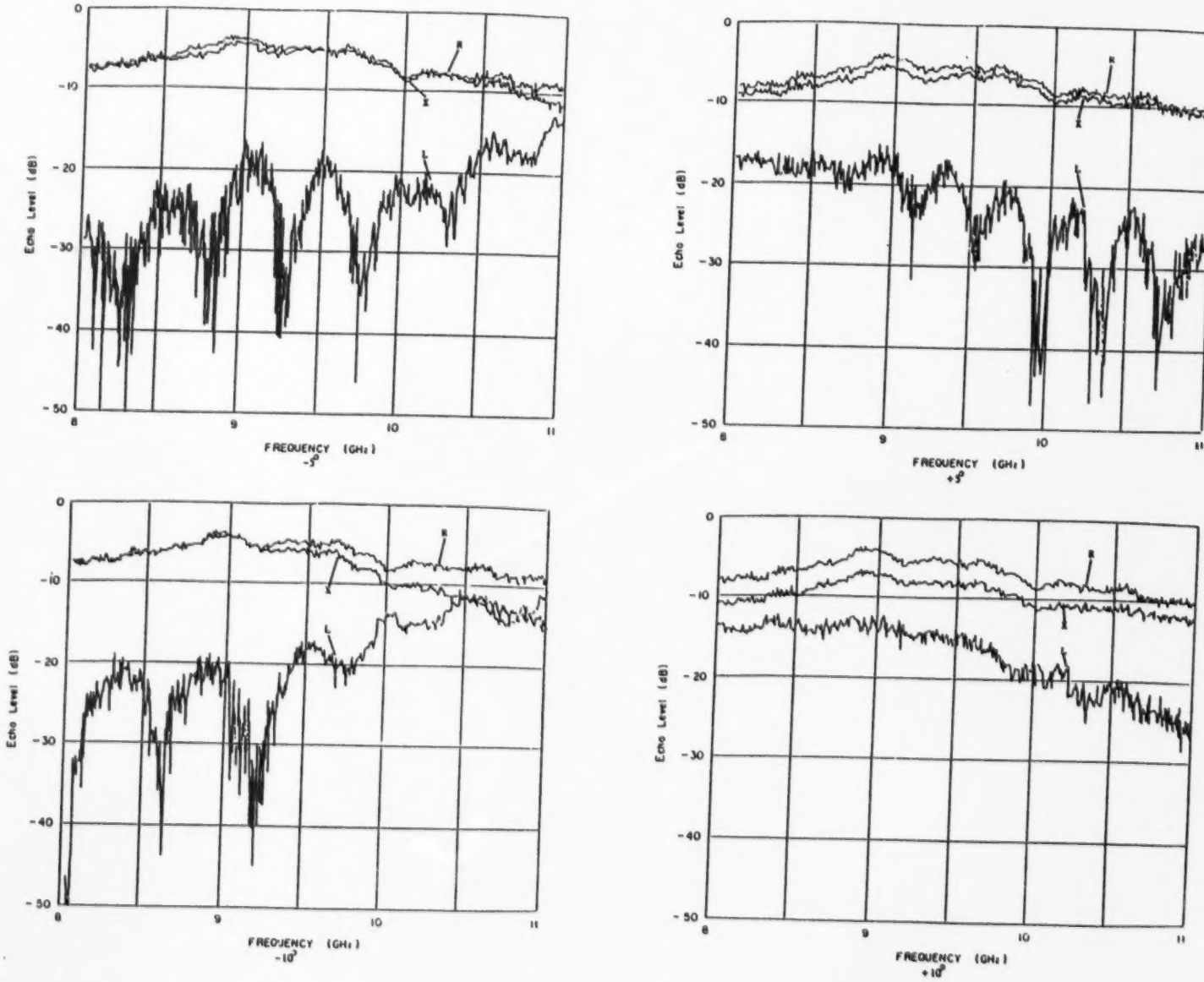

Figure 17 Reflector Signal as a Function of Elevation

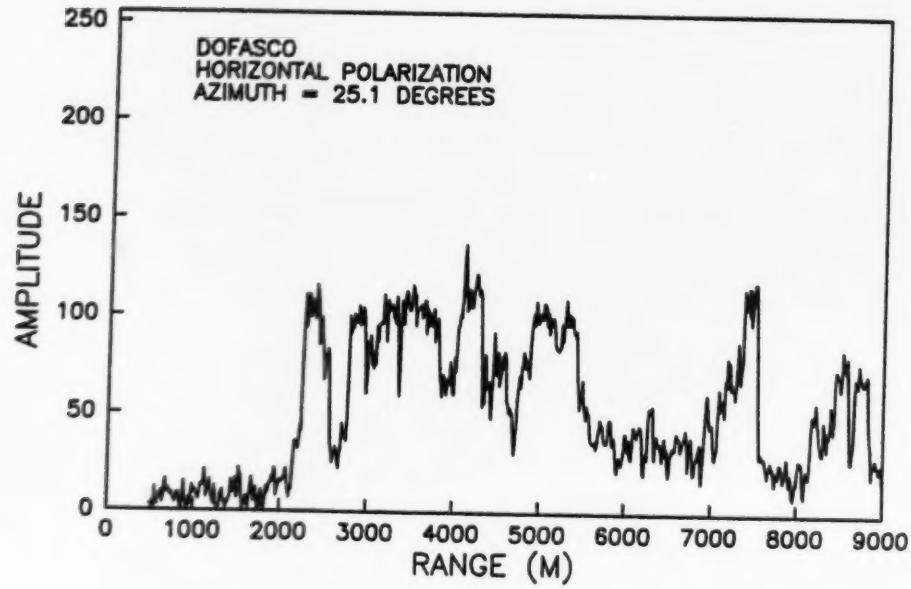

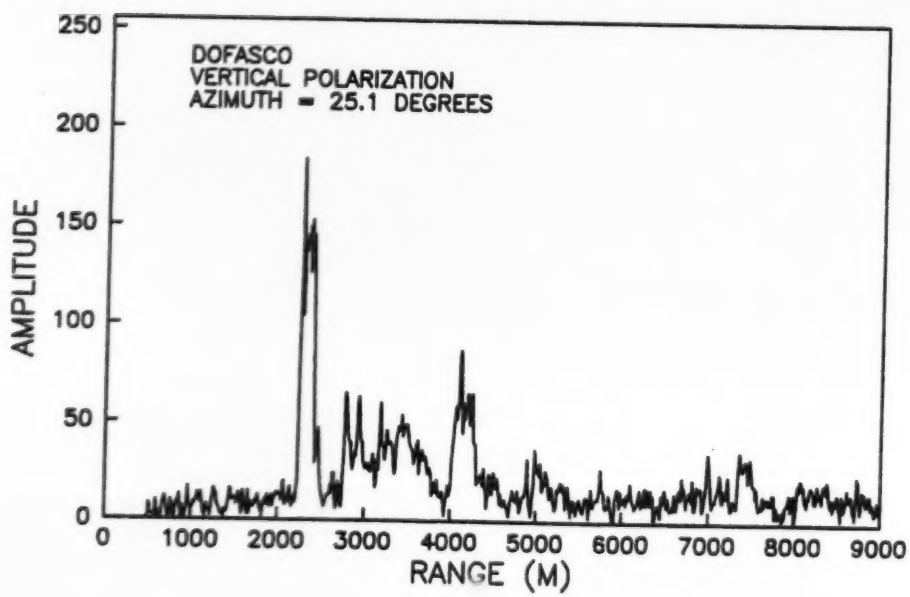

Figure 18 Horizontally and Vertically Polarized Sweeps of the Dofasco Reflector

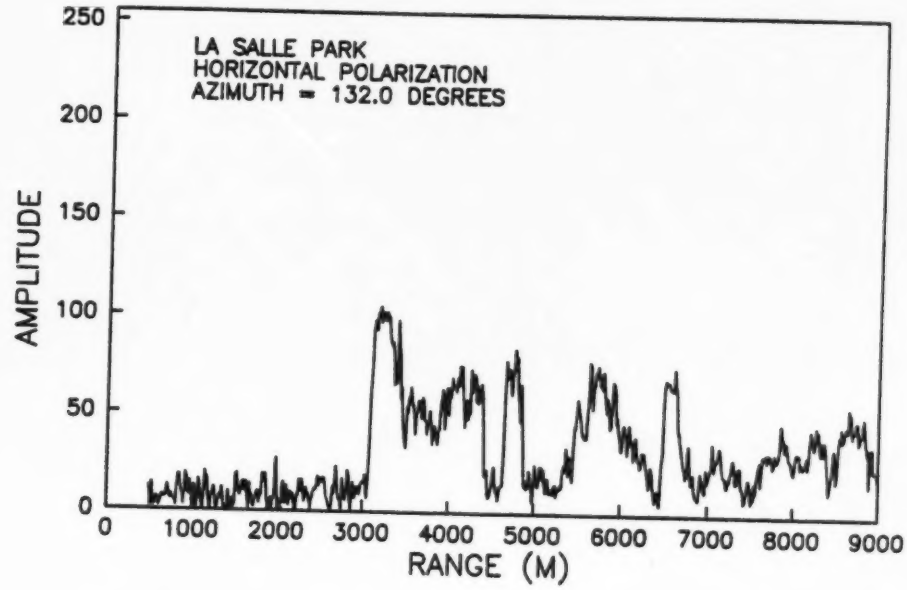

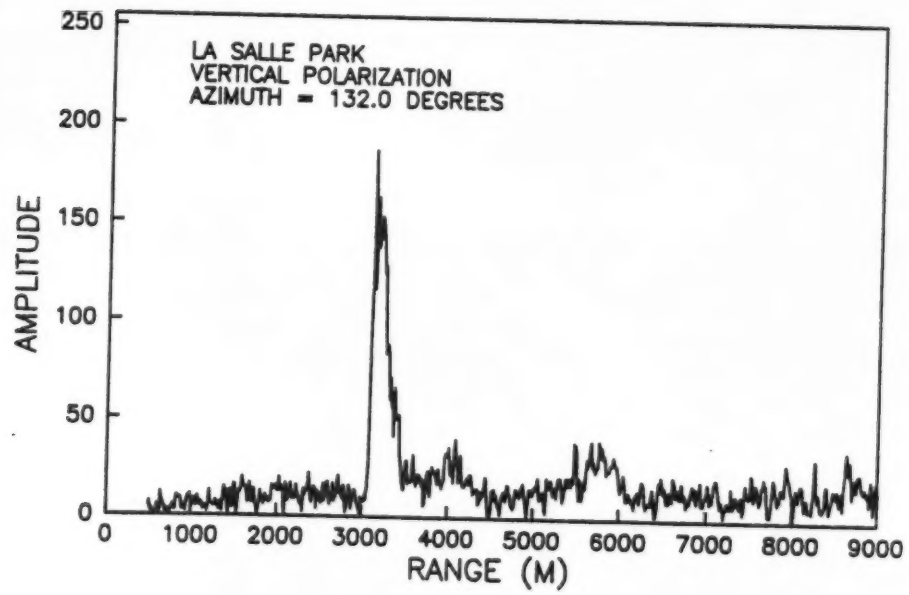

Figure 19 Horizontally and Vertically Polarized Sweeps of the La Salle Park Reflector

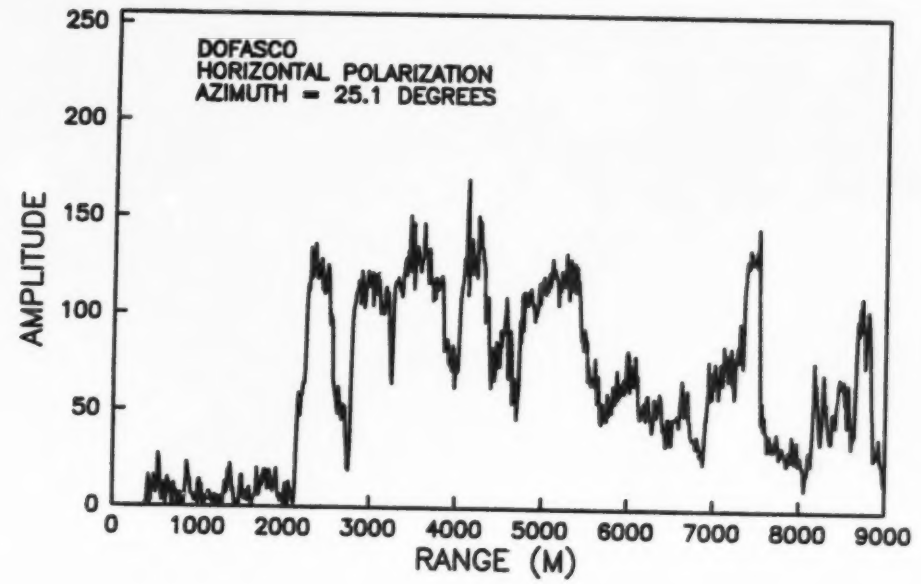

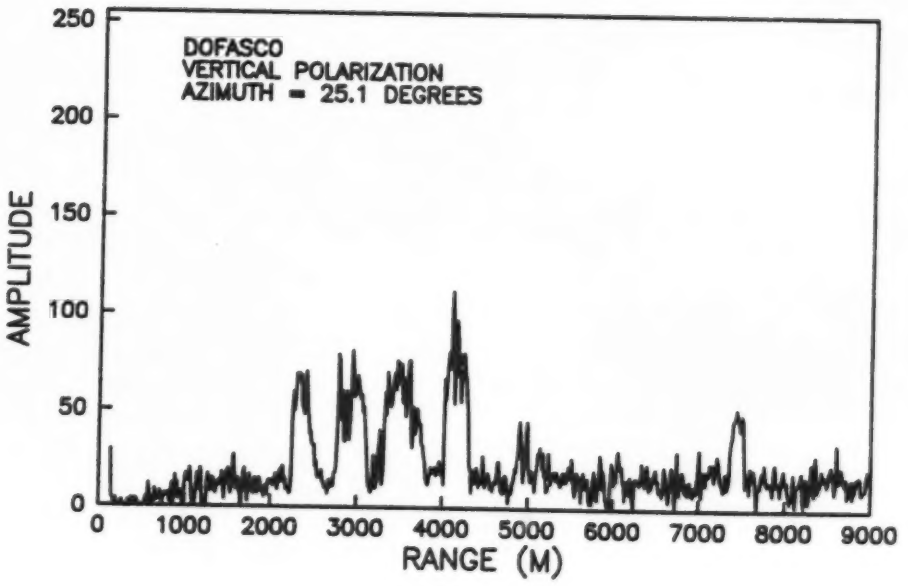

Figure 20 Horizontally and Vertically Polarized Sweeps of the Dofasco Site (No Reflector)

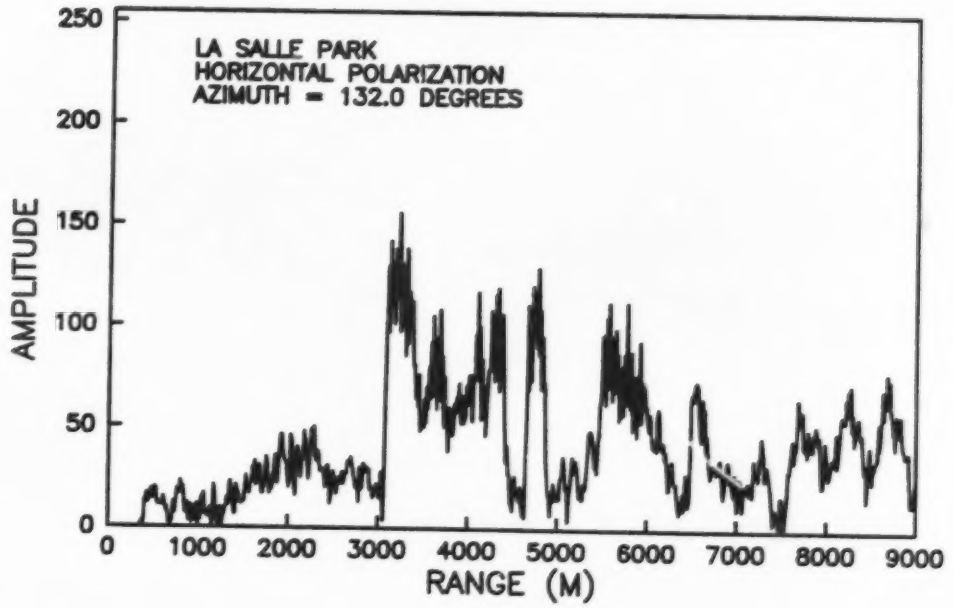

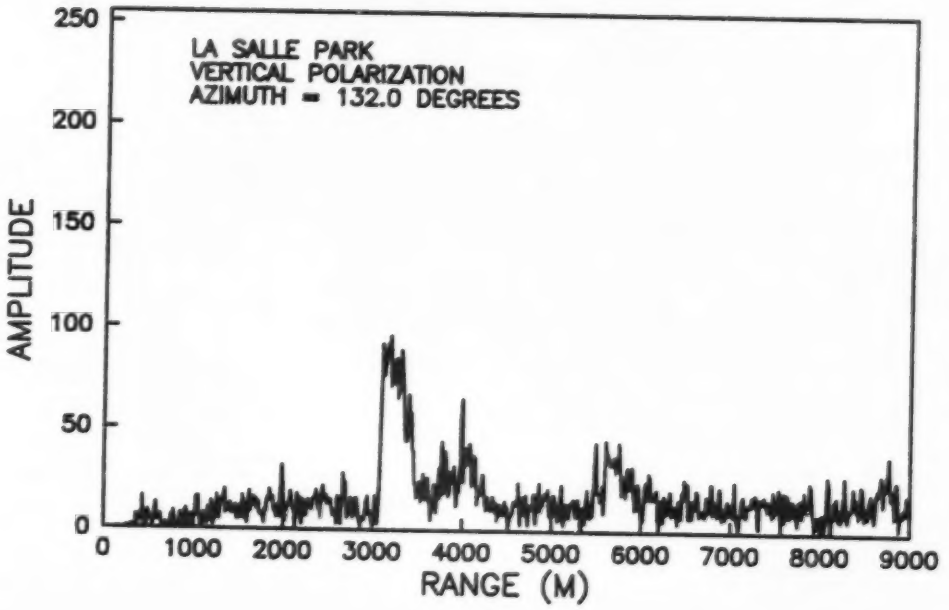

Figure 21 Horizontally and Vertically Polarized Sweeps of the La Salle Park Site (No Reflector)

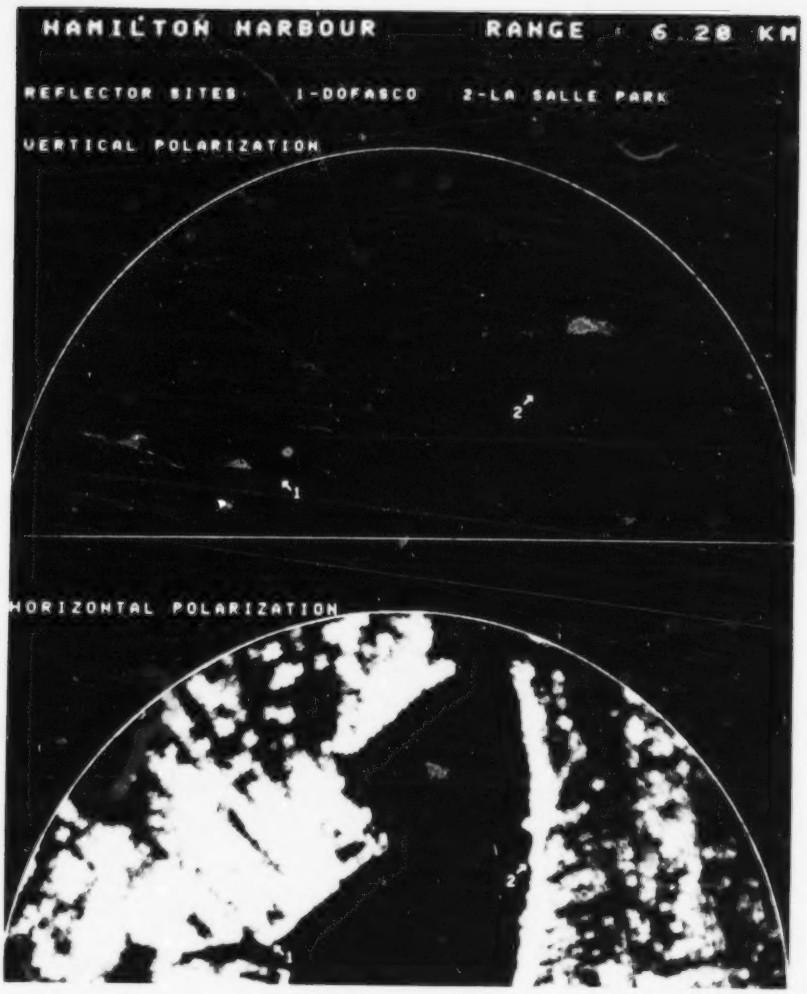

Figure 22 Scan Converted Image of Radar Coverage Area (Range=6.20 Km)

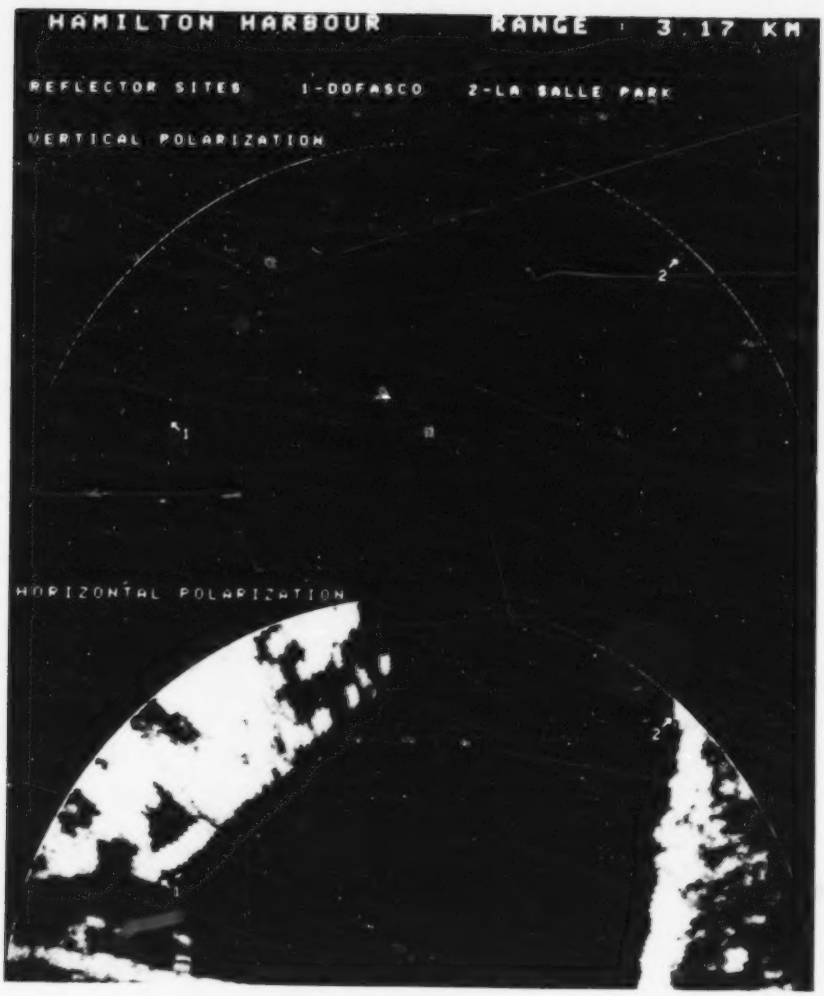

Figure 23 Scan Converted Image of Radar Coverage Area (Range=3.17 Km)

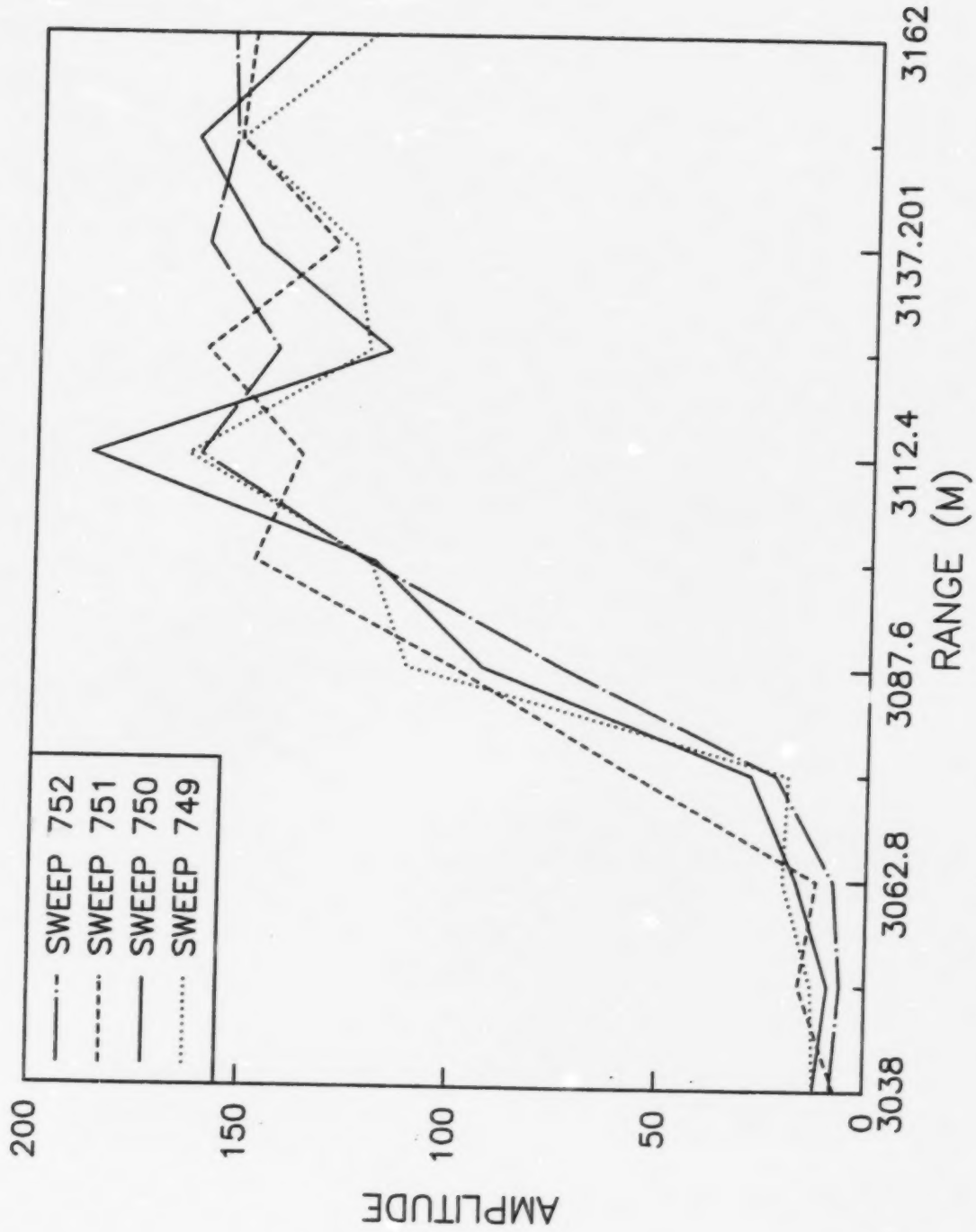

Figure 24 Target Detection: Vertical Sweeps of the La Salle Park Reflector Site

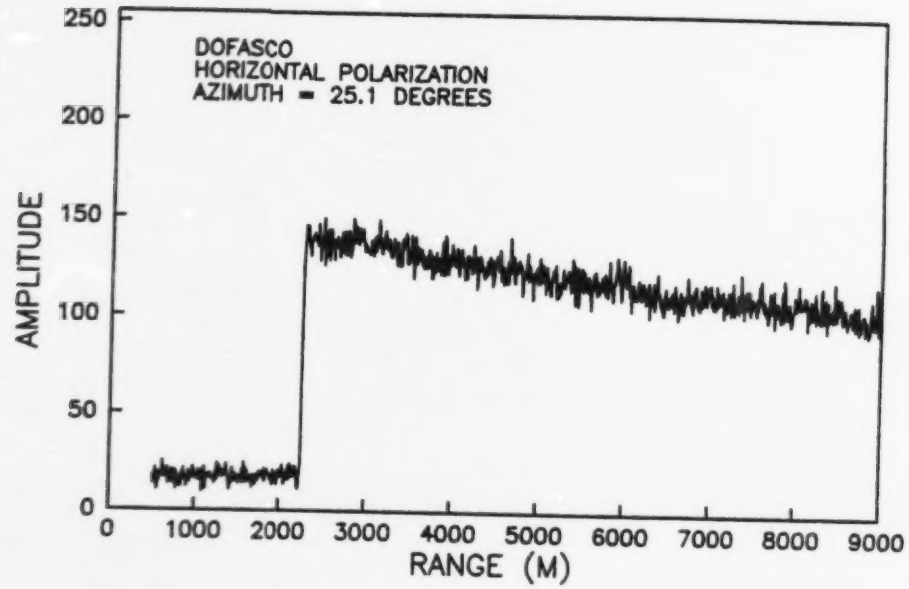

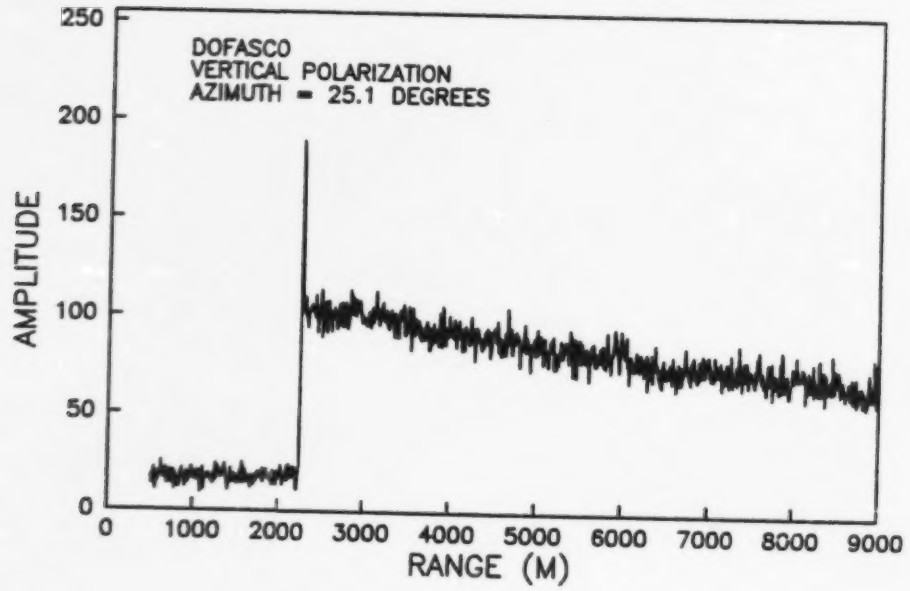

Figure 25 Simulated Sweeps of the Dofasco Reflector

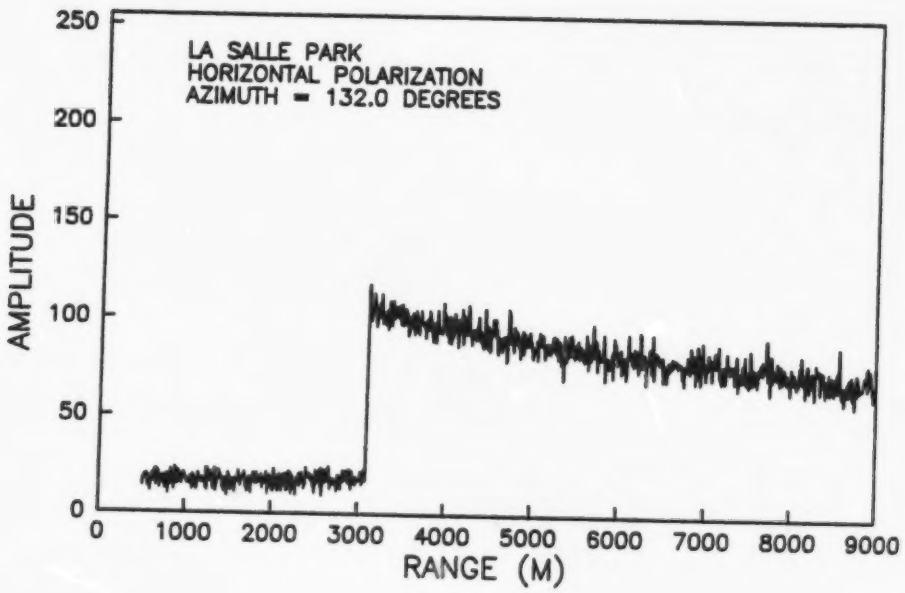

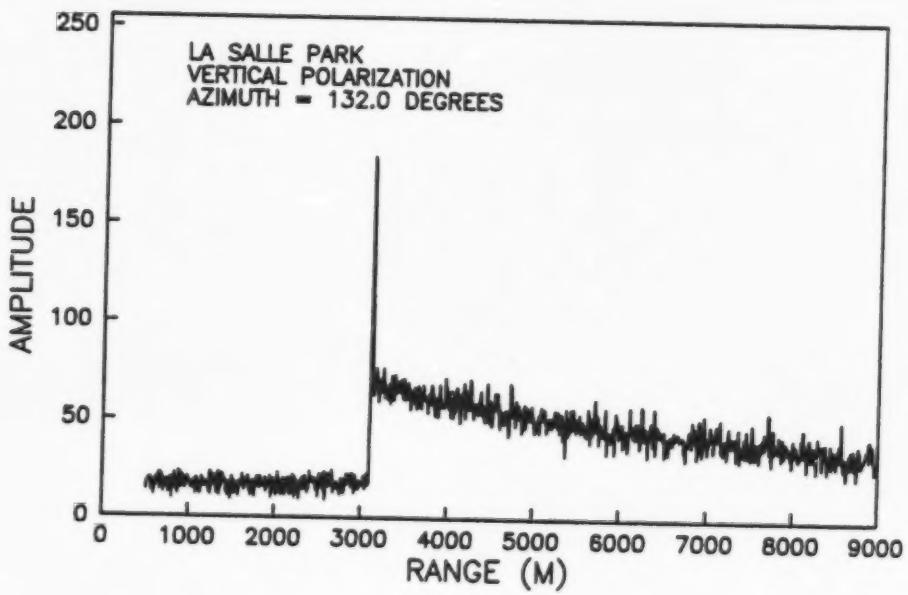

Figure 26 Simulated Sweeps of the La Salle Park Reflector

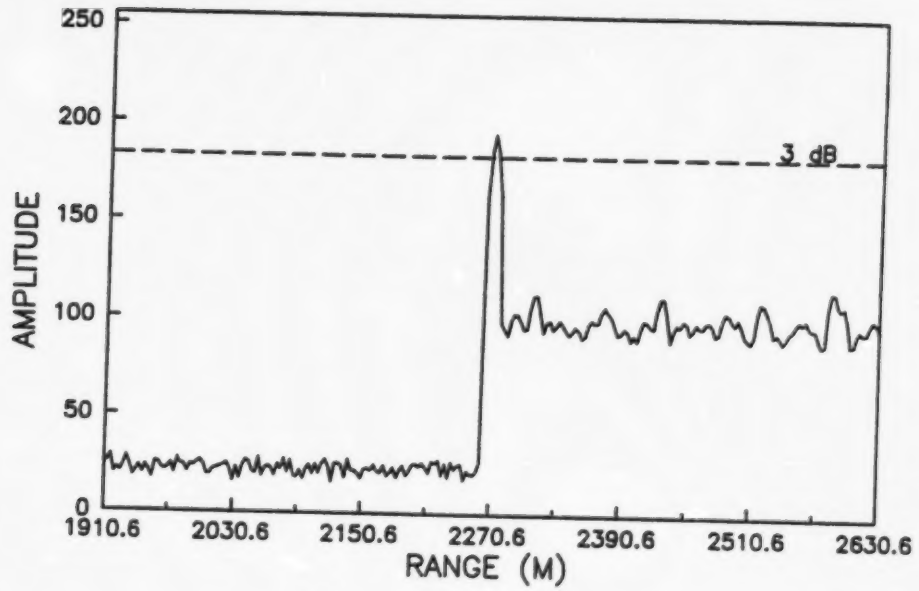

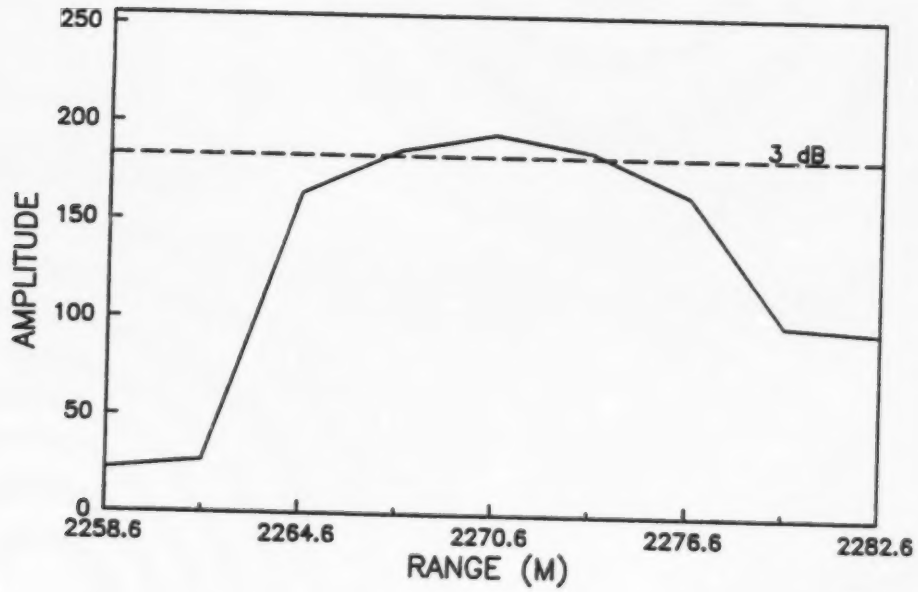

Figure 27 Range Accuracy Simulation

8. CONCLUSIONS

Based on the results presented in this report, we may state the following:

a. The twist grid reflector is capable of overcoming clutter in very hostile radar environments.

b. The scanning antenna can easily locate the reflectors in an operational environment.

c. Electromagnetic interference is not seen to be a problem to the operation of the system.

d. Reflector Parameters:
wire diameter = 0.045 mm
wire spacing = 5.5 mm
grid-reflector distance = 2.0 cm

e. Radar Parameters:
pulse width = 40 ns with a maximum rise time of 10 ns (for range accuracy of 7.5 m)
azimuth beamwidth = 1.5 to 2.0 degrees
elevation beamwidth = 15 to 20 degrees
pulse repetition frequency = 800 per second
antenna rotation rate = 30 rpm
isolation between feeds = 40 dB

In short, the Polarimetric Radar for Accurate Navigation (PRAN) system does provide a viable solution for automatic navigation along a confined waterway. Indeed, the stage is set for the development of a prototype version of the system for trials on board a ship.

REFERENCES

1. 'An Evaluation of a Precise Radar Navigation System', TDC Report TP 2800, Dominion Marine Association, Ottawa, Ontario, October, 1981.

2. Hope, A., 'Evaluation of a Precise Radar Navigation System (PRANS)', TDC Report TP 2980, Transportation Development Centre, August, 1981.

3. Miles, M.D., 'Phase I Evaluation of the ACCI PRANS Precise Radar Navigation System', NRC Report LTR-SH-282, Marine Dynamics and Ship Laboratory, National Research Council of Canada, September, 1981.

4. Greenlay, T. and Haykin, S., 'On the Design of Passive Retro-Reflectors for use with Precise Radar Navigation Systems', TDC Report TP 4507, McMaster University, April, 1983.

5. Macikunas, A., Haykin, S. and Greenlay, T., patent application, Oakville, Ontario, November, 1983.

6. Macikunas, A., 'Passive Polarimetric Reflector for Precise Radar Navigation', M. Eng. Thesis, March, 1985.

7. Fisher, E.T., 'Precise Navigation System, Operational Requirements', TDC Report, Transportation Development Centre, March, 1984.

8. Bird, G.J.A., 'Radar Precision and Resolution', Halsted Press, Wiley & Sons, New York, 1974.

LIST OF ABBREVIATIONS

ACCI	Associated Controls & Communications, Inc.
AP	array processor
CCIW	Canada Centre for Inland Waters
cm	centimetre
CRL	Communications Research Laboratory
dB	decibel
deg	degree
DMA	Dominion Marine Association
FPS	Floating Point System
GHz	gigahertz
GPIOP	general programmable input-output processor
HP	Hewlett Packard
KHz	kilohertz
Km	kilometre
LPRR	like polarization rejection ratio
m	metre
MHz	megahertz
mm	millimetre
MSE	mean square error
ns	nanosecond
PRAN	Polarimetric Radar for Accurate Navigation
PRANS	Precise Radar Navigation System
PRF	pulse repetition frequency
RCS	radar cross-section
rpm	revolutions per minute
SNR	signal-to-noise ratio
TDC	Transportation Development Centre

BIBLIOGRAPHY

Nathanson, F.E., 'Radar Design Principles', McGraw-Hill Book Company, New York, 1969.

Skolnik, M.I., 'Introduction to Radar Systems', McGraw-Hill Book Company, New York, 1980.